UC Davis

UC Davis Previously Published Works

Title

Strontium and oxygen isotopic profiles through 3km of hydrothermally altered oceanic crust in the Reykjanes Geothermal System, Iceland

Permalink

https://escholarship.org/uc/item/0f62k7gr

Authors

Marks, Naomi
Zierenberg, Robert A
Schiffman, Peter

Publication Date

2015-09-01

DOI

10.1016/j.chemgeo.2015.07.006

Peer reviewed

Strontium and oxygen isotopic profiles through 3 km of hydrothermally altered oceanic crust in the Reykjanes Geothermal System, Iceland

CrossMark

Naomi Marks *, Robert A. Zierenberg, Peter Schiffman

Department of Geology, University of California, Davis, CA 95616, USA

ABSTRACT

The Iceland Deep Drilling Program well RN-17 was drilled 3 km into a section of hydrothermally altered basaltic crust in the Reykjanes geothermal system in Iceland. The system is located on the landward extension of the Mid-Atlantic Ridge, and the circulating hydrothermal fluid is modified seawater, making Reykjanes a useful analog for mid-oceanic ridge hydrothermal systems. We have determined whole-rock Sr and O isotope compositions, and Sr isotope compositions of epidote grains from the RN-17 cuttings and RN-17B core. Whole rock oxygen isotope ratios range from -0.13 to 3.61‰ V-SMOW, and are isotopically lighter than fresh MORB (5.8 ± 0.2‰). The concentrations of Sr in the altered basalt range from well below to well above concentrations in fresh rock, and appear to be strongly correlated with the dominant alteration mineralogy. Whole rock Sr isotope ratios ranged from 0.70329 in the least altered crystalline basalt, to 0.70609 in the most altered hyaloclastite samples; there is no correlation with depth. Sr isotope ratios in epidote grains measured by laser ablation MC-ICP-MS ranged from 0.70360 to 0.70731. Three depth intervals, at 1000 m, 1350 m, and 1650 m depth, have distinctive isotopic signatures, where $^{87}Sr/^{86}Sr$ ratios are elevated (mean value > 0.7050) relative to background levels (mean altered basalt value ~0.7042). These areas are proximal to geothermal feed zones, and the 1350 m interval directly overlies the transition from dominantly extrusive to dominantly intrusive lithologies. Oxygen isotope measurements yield integrated water/rock ratios of 0.4 to 4.3, and suggest that hydrothermal fluids must have formerly had a component of meteoric water. Strontium isotopic measurements provide a more sensitive indication of seawater interaction and require significant exchange with seawater strontium. Both isotopic systems indicate that the greenschist-altered basalts were in equilibrium with hydrothermal fluids at a relatively high mean water/rock (Wt.) ratio ranging from about 0.5 to 4. These ratios are higher than estimates from ODP Hole 504B and IODP Hole 1256D, but are consistent with values inferred from vent fluids from 21° and 13°N on the East Pacific Rise (Albarède et al., 1981; Michard et al., 1984; Alt et al., 1996; Harris et al., 2015).

© 2015 Elsevier B.V. All rights reserved.

1. Introduction

Hydrothermal circulation at mid-ocean ridges modifies the thermal and igneous structures of oceanic crust, and exerts a major influence on the geochemical composition of the crust and oceans. Coupled fluid flow and chemical exchange act to cool the oceanic lithosphere and modulate the chemistry of the crust and oceans (e.g. Mottl, 2003). Despite the significance of hydrothermal circulation to global geochemical cycles, fundamental uncertainties in the magnitude of the fluxes remain. Although the magnitude of high temperature flux is reasonably well constrained from thermal modeling and geochemical budget approaches, the geochemical exchange mechanisms, and the structural, temporal, and spatial evolution of these systems remain unclear (e.g. Elderfield and Schultz, 1996; Davis et al., 2003; Mottl, 2003).

The Reykjanes geothermal system is analogous to mid-oceanic ridges in many ways, both in terms of secondary mineralization, hydrothermal solution, and primary lithology (Mottl and Holland, 1978). The Reykjanes geothermal field is a basalt-hosted, seawater-driven geothermal upflow zone and is situated on the landward extension of the Mid-Atlantic Ridge. The system lacks the shallow magma chambers such as those that have been imaged at a number of fast and intermediate spreading ridges, and in this way is similar to submarine portions of the slow spreading Mid-Atlantic Ridge (Cannat, 1993; Singh et al., 2006). Despite these obvious similarities, there are a number of important differences as well. Seismological studies model crustal thickness under Iceland of 10–40 km; the thinnest crust is associated with the volcanic zones of the Reykjanes Peninsula (Bjarnason et al. 1993; Staples et al. 1997; Darbyshire et al., 1998; Menke, 1999). The crustal thickness of the Iceland Plateau is therefore much greater than along normal, non-plume influenced portions of oceanic crust. Although the crustal thickness and architecture at the Reykjanes Peninsula differ from normal oceanic crust, the reaction of seawater with basaltic rocks occurs over a similar range in temperature, resulting in fluids

* Corresponding author at: Lawrence Livermore National Laboratory, 7000 East Avenue, Livermore, CA 94550, USA.
E-mail address: marks23@llnl.gov (N. Marks).

that are compositionally similar to seafloor black smoker fluids (Mottl and Holland, 1978; Hardardóttir et al., 2009). The concentrations of Cu, Zn, and Pb in the high-temperature reservoir liquids at Reykjanes are similar to those in the highest-temperature black smoker discharges; fluids discharged at the surface from the same wells have orders of magnitude lower metal concentrations due to precipitation caused by boiling and vapor loss during depressurization (Mottl and Holland, 1978; Hardardóttir et al., 2009). The Reykjanes geothermal system nevertheless represents a convenient analog for the study of water/rock interaction with implications for hydrothermal circulation through the mid-ocean ridges.

The extent of alteration and isotopic exchange in the crustal profile of the Reykjanes geothermal system provides important constraints on hydrothermal exchange in an active, basalt-hosted hydrothermal system. In this paper we present Sr isotopic and $\delta^{18}O$ alteration profiles in a ~3 km section of oceanic crust drilled at Reykjanes on the landward extension of the Mid-Atlantic Ridge in Iceland. The data represent continuous downhole profiles of $\delta^{18}O$ and Sr isotopic variation, from the high temperature reaction zone to the point of discharge. We argue that both meteoric water and seawater have been involved in developing alteration in the Reykjanes system. We demonstrate that the extent of isotopic exchange and water/rock ratios are similar to those observed in previously drilled in-situ oceanic crust. We conclude that water/rock ratios are limited by the number of assumptions upon which they are based, but find that ratios determined from two isotopic systems in RN-17 appear consistent with the values derived for submarine hydrothermal upflow zones.

2. Geologic background

The Reykjanes geothermal system is located on the southwestern tip of the Reykjanes Peninsula (Fig. 1). It is bounded by permeable fractures and faults forming a SW–NE trending graben-zone that is the sub-aerial continuation of the Reykjanes Ridge (Björnsson et al., 1970). The system is located within the highly permeable Holocene and Pleistocene formations of the Reykjanes Volcanic Belt and occurs in the westernmost portion of Iceland's Western Volcanic Zone (Björnsson et al., 1970). Unlike most Icelandic geothermal systems, and also most seafloor hydrothermal systems, shallow (1–3 km) magma chambers have not formed beneath the Reykjanes peninsula (Arnórsson, 1995 and references therein). Instead, fissure eruptions appear to be fed directly from magma reservoirs within the mantle (Gudmundsson, 1986, 1987, 1990).

The near-surface rocks at the Reykjanes geothermal system are Holocene basalt flows (the last known eruption occurred around 1240 AD) and Pleistocene subglacial hyaloclastites (Hreinsdóttir et al., 2001; Jóhannesson, 1989). At depth, submarine hyaloclastites and basalt flows are intercalated with marine sediments; submarine pillow basalt, basaltic breccias, and massive basalt flows overlie intrusive dikes (Fridleifsson et al., 2003). Feed zones, or permeable levels within the geothermal reservoir, frequently occur at the interface between different lithologies, and along the margins of intrusive dikes.

Reykjanes is a mature geothermal system that appears to have had a complex hydrothermal history. Evidence exists for evolving fluid compositions based on δD and $\delta^{18}O$ isotope ratios in the geothermal fluids (Sveinbjornsdottir et al., 1986; Pope et al., 2009), and variable salinity in fluid inclusions hosted by hydrothermal alteration minerals (Franzson et al., 2002; Fowler et al., 2015). During the Pleistocene glaciation, the Reykjanes Peninsula was covered by a continental ice sheet approximately up to 1100 m thick (Bourgeois et al., 2000) and ice extended approximately 100 km seaward down the Reykjanes Ridge from the present day shoreline (Hubbard et al., 2006). The Reykjanes geothermal system was dominated by meteoric fluids during this time (Franzson et al., 2002) and the increased load of the icesheet resulted in high fluid pressures, and therefore a shallower boiling depth in the Pleistocene (Marks et al., 2010; Franzson et al., 2002). The occurrence of high temperature alteration phases at shallow depths

within the well (e.g. epidote at 350 m) implies much higher pressures and temperatures in the past (e.g. Marks et al., 2010; Franzson et al., 2002).

Following the retreat of the icesheet at the end of the last glacial maximum, seawater began to be the dominant hydrothermal fluid in the system, as it is today. Interaction between alteration phases formed during the early, meteoric-water dominated hydrothermal regime and modern hydrothermal fluids result in a geothermal fluid with depleted δD values of −21‰, a value intermediate between modern seawater $\delta D = 0‰$, and Pleistocene ice sheet derived water ~−120‰ (e.g. Pope et al., 2009). The δD and $\delta^{18}O$ isotope compositions and compositional zoning of secondary minerals reflect these changes in hydrothermal fluid composition (Pope et al., 2009). A cartoon depicting the glacial evolution of the Reykjanes geothermal system is shown in Fig. 2.

2.1. The Iceland Deep Drilling Program and RN-17

The major aim of the of the Iceland Deep Drilling Program is to investigate an active subcritical to supercritical transition in oceanic crust in order to determine the pressures, temperatures, and fluid compositions of a supercritical geothermal system in support of enhanced geothermal energy production. The Reykjanes geothermal system was selected for investigation because the geothermal fluid is modified seawater; the elevated salinity raises the critical temperature of the Reykjanes fluid to approximately 410 °C (Bischoff and Rosenbauer, 1984; Fridleifsson et al., 2003). Well RN-17 is sited on the flank of the Reykjanes geothermal system and was designed to reach supercritical fluids at about 4 km depth, although these depths were not reached during the first phases of drilling.

The samples for this study are drill cuttings from well RN-17 and core from RN-17B, a sidetrack boring kicked off from RN-17 at 920 m and directionally drilled towards the south at ~30° from horizontal to a total depth of 3078 m. The boreholes are located on the southern flank of the geothermal field at Reykjanes at 63°49′12″N, 22°41′24″W (Fig. 1). RN-17 was drilled to a depth of 3082.4 m between September 2004 and January 2005. Sidetrack RN-17B, was completed in 2008 to a total depth of 3078 m. RN-17B was cored over a 9 m interval (2798.5–2808.5 m); core recovery was 100%. Cuttings from each well were continuously collected and sampled at 2 m intervals, except at the noted feed points where loss of circulation of drilling fluids prevented recovery. The cuttings studied in this present work are from RN-17; the core studied is from RN-17B. A brief description of the lithology follows. The first submarine lavas are pillow basalts encountered at 368 m in RN-17. Marine sediments occur between 390–472 m and 516–720 m and comprise sandy silts and reworked tuff sediments; fragments of marine fossils occur in these cuttings as well. These sediments intervals constitute a minor part of the stratigraphy and tend to be intercalated with volcaniclastics and reworked tuffs. The first intrusive igneous rocks occur in a sequence of at least 30 dike units at 1390 m. These dikes intrude into hyaloclastites and pillow basalt sequences (Fridleifsson et al., 2005). Downhole mineralogical and geochemical trends, based on examination of cuttings at approximately 50-meter intervals, are discussed in Marks et al. (2010) and Marks et al. (2011).

Cuttings and core from RN-17 and RN-17B include crystalline basalts, hyaloclastites, basaltic tuffs and breccias (Fig. 3). These basaltic rocks are primarily tholeiites clustered around the Enriched-Mid-Ocean Ridge Basalt (E-MORB) composition (Marks et al., 2010), and are in good agreement with the compositional range of published data on Icelandic and Reykjanes Ridge basalt (Hemond et al., 1993; Murton et al., 2002; Stracke et al., 2003; Kokfelt et al., 2006; Pearce, 2008). The crystalline basalts contain ophitic plagioclase and augite with accessory titanomagnetite and Cr-spinel. Primary igneous olivine phenocrysts, almost universally altered to chlorite or chlorite-smectite, make up 1–2% of the rocks. Hyaloclastites, breccias, and tuffs originally included quenched plagioclase and augite as well as basaltic glass.
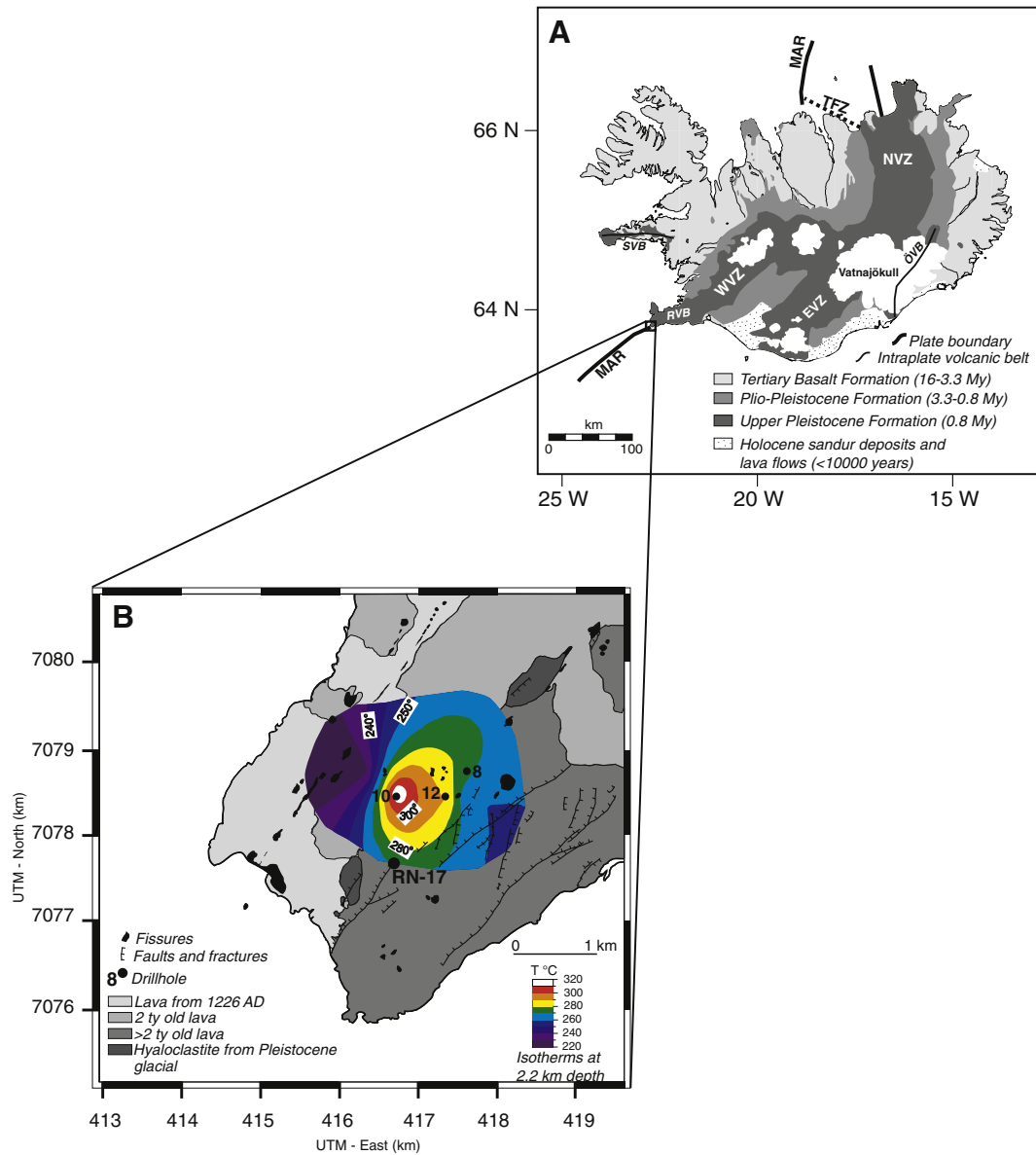
Fig. 1. (A) The principal elements of the geology of Iceland outlining the distributions of the major geological subdivisions, including the main fault structure and volcanic zone and belts: MAR = Mid-Atlantic Ridge; RVB = Reykjanes volcanic belt; EVZ = Eastern volcanic zone; WVZ = Western volcanic zone; NVZ = Northern volcanic zone; TFZ = Tjörnes fault zone; OVB = Öraefi Volcanic Belt; SVB = Snaefellsnes Volcanic Belt. (Modified after Thordarson and Larsen, 2007). (B) Map of the Reykjanes Peninsula showing major faults, fractures, Holocene lava flows and fissure swarms, and the location of RN-17 and RN-17B; temperature isotherms of wells at 2.2 km depth are designated by shading, isotherm contour interval = 10 °C and are based on measurements from approximately 25 wells drilled into the geothermal field. (Modified from Franzson et al., 2002; Fridleifsson et al., 2003; Pope et al., 2009, and Marks et al., 2011).

All of the cuttings contain at least some alteration, although crystalline basalts are generally far less altered (5–10% altered) than the hyaloclastites and breccias (70–80% altered). Primary igneous phases are variably replaced by hydrothermal minerals in the following ubiquitous assemblages, and are presented graphically in Fig. 3. Primary igneous plagioclase is slightly to totally recrystallized to albite, and somewhat less commonly altered to potassium feldspar below 1800 m in the well. Igneous augite is partly to totally replaced by chlorite or amphibole, often with included magnetite blebs and fine-grained titanite. Primary olivine is almost totally replaced by chlorite, mixed-layer chlorite–smectite, and smectite, although rare relict olivine is present in some of the least altered rocks. Epidote occurs in veins, as well as in amygdale filings, and replacing feldspar. Andradite garnet occurs primarily as small (50 um) porphyroblasts within amygdales associated with chlorite and epidote. Amphibole ranges in composition from actinolite to magnesiohornblende. The alteration phases in cuttings

below about 500 m depth are indicative of greenschist facies metamorphic conditions. Cuttings from the 2150 m and 2650 to 2850 m depths contain rare granoblastic grains comprising calcic plagioclase, quartz, clinopyroxene, orthopyroxene, and olivine as well as cordierite and spinel. These grains are interpreted to result from contact metamorphism imposed on the dominantly greenschist facies altered basalts resulting from the intrusion of dikes (Marks et al., 2011). Peak metamorphic temperatures derived from 2-pyroxene geothermometry (Andersen and Lindsley, 1988) indicate temperatures as high as 967 °C (Marks et al., 2011).

The core from RN-17B includes units of homolithic and heterolithic hyaloclastite breccias, volcanic sand, and crystalline basalt with quench texture. The core is highly altered (80–90% recrystallized) and includes patches of light and dark alteration. The darker alteration patches are dominantly altered to massive felted actinolite/hornblende and disseminated chlorite, epidote and albite. Lighter patches are dominated by
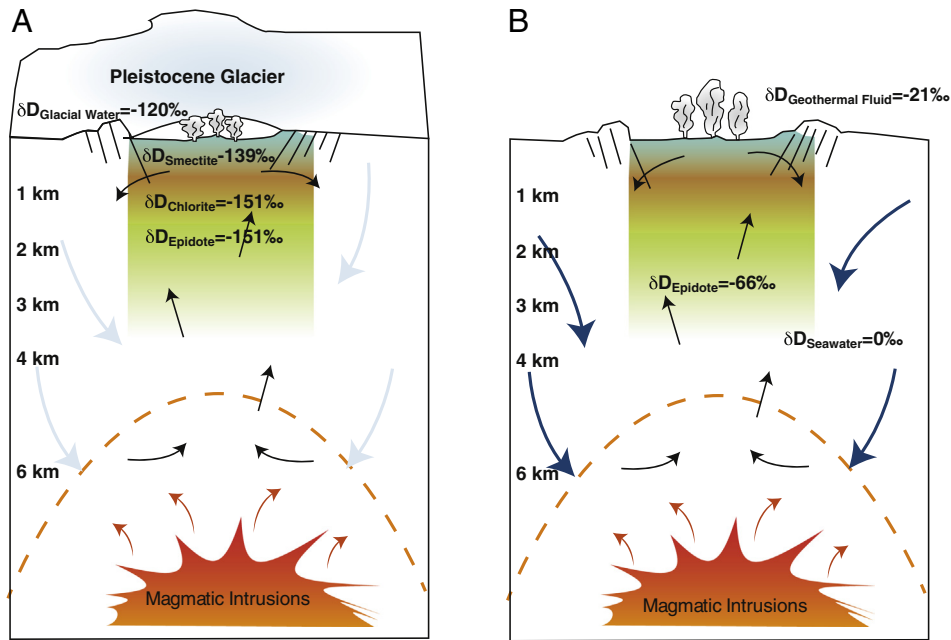
Fig. 2. A) Schematic model of the early Reykjanes geothermal system, which was overlaid by 1.5 to 2 km thick ice sheet that extended laterally as much as 50 to 100 km from the Reykjanes peninsula. The hydrothermal fluids were ice-sheet derived meteoric water. The presence of this ice sheet would also have caused higher pore pressures in the system, thereby raising the boiling point with depth curve in the system and shifting the precipitation of high temperature alteration phases shallower in the system (i.e. Marks et al., 2010; Bargar and Fournier, 1988) B) the modern Reykjanes system lacks the glacial overburden, and as a result the hydrothermal fluids are derived from seawater. The modern geothermal fluid interacts with relict hydrous minerals in ithe upflow zone, and this causes the geothermal fluids to have their distinct isotopic composition that matches neither present day meteoric water δD values, Reykjanes basalt values, nor seawater δD values.
Figure modified after Pope et al., 2009.

epidote and albite. Amygdales are filled with epidote and pyrite, as well as albite, and actinolite/hornblende. The core is cut by numerous veins of epidote + pyrite, anorthite + actinolite/hornblende + epidote + chlorite, and epidote + actinolite/hornblende. The RN-17B core appears more altered than cuttings from similar depth, and this may reflect preferential recovery of less altered lithologies in the cuttings returned to the surface during rotary drilling.

The alteration phases form a prograde hydrothermal alteration sequence with depth (Lonker et al., 1993; Franzson et al., 2002; Fridleifsson et al., 2005; Marks et al., 2010). Alteration zones in the Reykjanes system have been defined by the presence of one or more index minerals (Tómasson and Kristmannsdóttir, 1972; Franzson et al., 2002). In order of increasing alteration grade the zones are as follows: smectite–zeolite, epidote-mixed-layer clay, chlorite–epidote, epidote–actinolite, and amphibole zones (Lonker et al., 1993; Franzson et al., 2002; Fridleifsson et al., 2005; Marks et al., 2010) (Fig. 3). The temperature profile measured in RN-17 following equilibration after drilling is included in Fig. 3, and provides a constraint on the conditions of isotopic fractionation presented below.

3. Analytical procedures

The samples studied are drill cuttings from the 3082 m deep RN-17 as well as three samples of core from the RN-17B (2798.5–2808.5 m) sidetrack. Cuttings ranged in size from 1 to 5 mm in diameter. Thirty-six samples for whole-rock isotopic analysis were selected from drill cuttings at intervals designed to be representative of the range of alteration observed, generally at 50 to 100 m depth intervals (Marks et al., 2010). Three samples from the RN-17B core were selected to be representative of the range of alteration observed in the core. Core samples were manually powdered in a synthetic sapphire mortar and pestle. Cuttings samples for isotopic analysis were pulverized in a tungsten carbide shatter-box. Epidote mineral separates were handpicked from RN-17 cuttings and mounted as polished sections. Thin section mounts were prepared for optical petrography and isotopic analysis and

analyzed at the UC Davis Interdisciplinary Center for Plasma Mass Spectrometry. In the RN-17 cuttings, epidote occurs as yellowish green, xenoblastic crystals (<0.8 mm) and also as radiating crystal aggregates (25–250 μm) commonly replacing plagioclase and filling vesicles and veins as a secondary alteration mineral.

Loss on ignition (LOI) was measured at the Peter Hooper GeoAnalytical Laboratory at Washington State University by heating the samples in ceramic crucibles to 900 °C overnight.

The concentration of Sr in epidote was determined by electron microprobe analysis using a CAMECA SX-100. Wavelength dispersive analyses were done at a 15 keV accelerating potential and a sample current of (100 nA). Wavelength dispersive peak and background times were 60 s. Sr was measured using the Sr Lα peak and an $Sr_2Al_2Si_2$ calibration standard with the LPET crystal. A one sided background offset to +800 sinθ was used in order to avoid the Si Kα peak. Strontium determinations are precise to ± 15% (2σ) of the amount present at concentrations between the detection limit (140 mg/kg) and 1000 mg/kg.

In-situ $^{87}Sr/^{86}Sr$ analyses of individual epidote grains were obtained using the Nu Plasma HR MC-ICP-MS coupled to a UP-213 laser ablation system equipped with an Nd:YAG deep UV (213 nm) laser (New Wave Research, USA) similar to the methods of Hobbs et al. (2005). Epidote grains were selected for ablation using a petrographic microscope, by first locating the grains in transmitted light, and then confirmed by SEM. A typical ablation track in epidote is shown in Fig. 4. Single spots in each epidote grain were assayed using a laser beam size of 95 μm, 100% laser power, and 20 Hz repetition rate. Typical ^{88}Sr signals of 0.5–5 V were obtained during the analyses. Helium was used as a carrier gas to maximize sensitivity and minimize sample deposition at the ablation site, and mixed with Ar after the laser sample cell but before sending the aerosols to the plasma source. Gas blank and background signals were monitored until ^{84}Kr and ^{86}Kr were stable after each sample change, which required exposing the sample cell to air, and measured for 30 s. Samples were ablated for 30–60 s. Background was subtracted from the measured signals automatically. The $^{86}Sr/^{88}Sr = 0.1194$ was used to correct for instrumental fractionation with the exponential
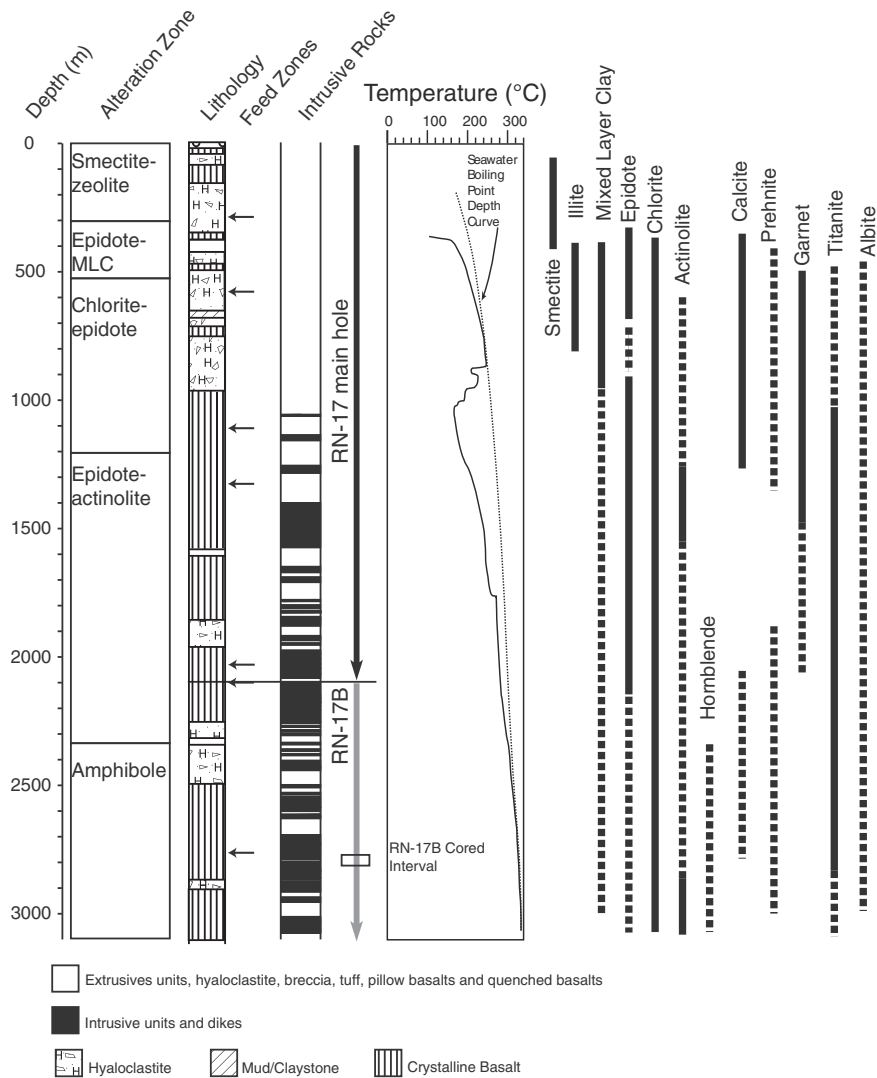
Fig. 3. Alteration zones, lithology, feed points, and formation temperature profile in RN-17. RN-17 and RN-17B are colocated wells, RN-17B is a sidetrack directionally drilled to the south at ~30° that kicks off from 2100 m in RN-17, as shown by the arrows. Formation temperatures were measured in the upper portion of RN-17 and in the sidetrack RN-17B (Marks et al., 2010) and are equilibrating towards the seawater boiling point with depth curve, indicated by the dashed line. Feed points are inferred from loss of circulation and temperature logs; all are considered to be minor. Mixed layer clays are abbreviated as MLC. The maximum downhole temperature is calculated from flow tests to be 370–380 °C.

law. Peak intensities for ^{88}Sr, ^{87}Sr, ^{86}Sr, ^{85}Rb, and ^{84}Sr were measured simultaneously. The ^{85}Rb peak was monitored to correct for ^{87}Rb interference on ^{87}Sr, which was negligible. The gas flow and electrostatic lens settings were optimized for maximum Sr sensitivity and peak-shape while ablating an in-house carbonate standard. An in-house carbonate standard (modern deep water coral) was used as a LA standard, giving an $^{87}Sr/^{86}Sr$ ratio equal to 0.709177 ± 8.

Strontium isotope compositions were determined on whole-rock samples by MC-ICP-MS at UC Davis. Approximately 100 mg of powdered sample underwent standard HF-HNO$_3$ dissolution. Sr was separated from the digested whole rock powers by Eichrom Sr-Spec resin. Samples were diluted with 0.1 M HNO$_3$ to ~0.5 mg/L Sr concentration to obtain optimal counting statistics for mass spectrometric analysis. Samples and standards were introduced into the Ar-plasma source of the MC-ICP-MS through a standard self-aspirating Meinhard nebulizer. The NIST Sr isotope standard SRM 987 was measured repeatedly during the course of this study with an average $^{87}Sr/^{86}Sr$ equal to 0.710253 ± 9.

Oxygen was extracted from whole rock powders at the Stable Isotope Biogeochemistry Laboratory at Stanford University. Oxygen isotopic measurements were conducted using infrared laser fluorination after Sharp (1990). Whole rock powders were compressed into ~1.5 mg pellets, placed in a nickel sample holder, and dried at vacuum

overnight to remove any sorbed fluids. Samples were heated using a CO$_2$-infrared laser in a vacuum chamber containing the oxidizing agent BrF$_5$ in the method after Sharp (1990). The oxygen gas released was directly analyzed using a dual-inlet Finnigan MAT-252 mass spectrometer. All isotopic analyses of oxygen are reported in standard δ-notation relative to V-SMOW (Vienna Standard Mean Ocean Water). Isotope compositions were corrected relative to UWG-2 garnet laboratory standard (Valley et al., 1995) with an average offset of less than 0.5‰.

4. Results

4.1. Oxygen isotopes

Whole rock samples from RN-17 and RN-17B have δ^{18}O values of −0.13‰ to 3.61‰ (Table 1) and are depleted in ^{18}O relative to unaltered basalt from the Reykjanes peninsula (δ^{18}O = 4.8–6.3‰ n = 15; Muehlenbachs et al., 1974; Hemond et al., 1988) or fresh Mid Atlantic Ridge MORB (δ^{18}O = 5.40–5.81‰, n = 15; Taylor, 1968; Muehlenbachs and Clayton, 1972; Eiler et al., 2000). Whole rock oxygen isotope values overlap those of epidote separates sampled from RN-17, which have δ^{18}O values of −0.1‰ to 2.3‰ (Pope et al., 2009). The
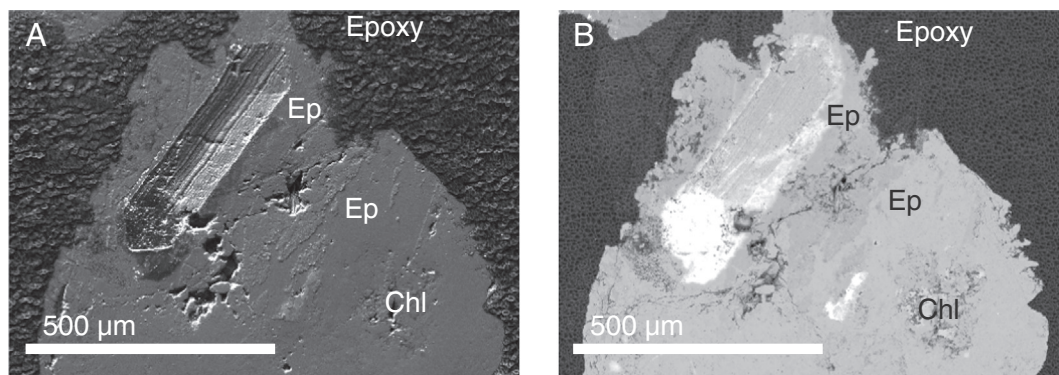
Fig. 4. In-situ measurements of [87]Sr/[86]Sr in epidote in veins and amygdales was accomplished by laser-ablation ICP-MS. Samples were aerosolized with a New Wave Research UP-213 laser ablation system. Targets for laser ablation were selected by optical microscope; the ablation paths were confirmed by SEM and EDS. Figure A shows the trace of the ablation path in SEM; Figure B shows a BSE image confirming homogeneity of the mineral grain; the bright white areas are locations where the carbon coat has been removed by the laser. Ep = epidote, Chl = chlorite.

oxygen isotope values from RN-17 do not show a systematic variation with depth (Fig. 5). Oxygen isotope values from whole-rock samples from the extensively altered RN-17B core are consistent with the epidote measurements, and more depleted than whole-rock values determined from cuttings (Fig. 5).

4.2. Sr isotope compositions and Sr concentrations of cuttings and core

Results of Sr isotopic analyses and Rb and Sr contents of whole-rock samples from RN-17 and RN-17B are presented in Table 1. Rubidium concentrations are low relative to Sr concentrations in these rocks (generally <0.1 mg/kg to 8 mg/kg Rb; N-MORB range 0.4–1.5 mg/kg Rb; Hart et al., 1999) and the rocks are young (<1 m.y.), so the age correction to the [87]Sr/[86]Sr ratio for Rb decay is insignificant.

Sr contents of the rocks range from 82 to 230 mg/kg, a range that brackets the average Sr composition of unaltered Reykjanes basalt (167 mg/kg, n = 27; Peate et al., 2009). Whole-rock Sr isotopic values range from 0.70329 to 0.70609 (Table 1). There is no discernable trend of [87]Sr/[86]Sr ratios with depth or alteration zone (Fig. 5). These values are slightly to significantly shifted towards seawater composition, although the lowest values of ~0.7033 are near the values reported for fresh basalt from the Reykjanes Peninsula (up to 0.70322 ± 7 2σ; Elderfield and Greaves, 1981; Fig. 6). The [87]Sr/[86]Sr composition is positively correlated with loss on ignition (LOI), although the Sr concentration in the rocks does not correlate with [87]Sr/[86]Sr (Fig. 7). Samples from 1000 and 1350 m fall off this trend, with [87]Sr/[86]Sr ratios > 0.705 and LOI of ~2.6. These samples are both from cuttings collected adjacent to inferred geothermal feed zones.

4.3. Concentration and Sr isotope composition of epidote

Epidote Sr contents range from 507 to 1638 mg/kg, with an average composition of 1020 mg/kg (n = 24) (Table 2). Epidote grains are zoned with respect to Sr concentration; many have more Sr-rich rims and less Sr-rich cores. Some individual epidote grains are zoned with respect to Sr isotopes as well, with cores generally less radiogenic than the rims (e.g. an epidote from 1000 m with a core of 0.70504 and a rim of 0.70731). There is no correlation between Sr content and [87]Sr/[86]Sr ratio across different epidote grains. Epidote grains do typically have higher Sr contents and higher [87]Sr/[86]Sr than the surrounding host rock (Fig. 7).

Strontium isotope ratios of epidote grains vary from 0.70360 to 0.70731 with a mean value of 0.70437 (n = 81 spots on a total of 59 different grains) (Table 2). There is no systematic change in epidote [87]Sr/[86]Sr with depth (Fig. 5). There is also no systematic variation with occurrence mode (i.e. void-filling v.s. replacement of plagioclase).

Epidote grains in cuttings from 1000 m, 1350 m, to 1650 m depth have elevated [87]Sr/[86]Sr ratios (mean value ~ 0.7056) relative to background levels (mean value ~ 0.7042). Epidote from 1000 m is hosted in basaltic breccia, and was located above a small feed zone (i.e. permeable region), identified by loss of circulation during drilling. Bulk-rock samples from 1000 m have slightly elevated LOI, K_2O, and Na_2O relative to the average alteration profile (Marks et al., 2010), suggesting increased alteration resulting from proximity to the feed zone. Epidote from 1350 m is hosted in glassy basalt, and was located just above a small feed zone. This unit occurs within the transition from extrusive to primarily intrusive lithologies, a transition that spans approximately 25 m. Samples from this depth have slightly elevated LOI and Na_2O, suggesting increased hydrothermal alteration. Epidote from 1650 m is hosted in crystalline basalt, the host rock does not show other geochemical evidence for enhanced alteration.

5. Discussion

5.1. Geochemical estimation of water/rock ratios — oxygen isotope constraints

We apply two approaches for calculating the water/rock ratios using O and Sr isotopic data. Calculated water/rock ratios are based on assumptions about 1) initial compositions of unaltered rock and hydrothermal fluid, 2) degree of exchange between liquid and solid phases, and 3) the closed or open nature of the system (Spooner et al., 1977; Mottl, 1983; Fisher, 1998). Because water/rock ratios estimated from rock chemistry are integrated over the life of the hydrothermal system, they may reflect multiple stages of alteration. Values estimated using different tracers tend to vary due to differing reaction kinetics. As a rule they are less than the absolute (physical) water/rock ratio because fluid residence times may be too short for attainment of geochemical equilibrium, and fluids will undoubtedly pass through previously altered rock (Fig. 8).

Oxygen isotope profiles through oceanic crust and ophiolites have been routinely interpreted in terms of water/rock exchange, as reviewed by Alt and Teagle, 2000. The oxygen isotope depth profile for Reykjanes shows significant depletion of [18]O similar to the sheeted dike and upper gabbroic section of oceanic crust and ophiolite sequences (Alt and Teagle, 2000 and contained references). The δ^{18}O values from Reykjanes are lower than most values reported from oceanic crust and ophiolites, and include some values less than 0‰. The depletion in oxygen isotopes has been interpreted as an indication of exchange between basaltic rocks and hydrothermal fluids at temperatures consistent with greenschist facies to lower amphibolite facies alteration minerals.

Table 1
Sr and O isotope compositions of bulk rock samples from RN-17 and RN-17B.

Borehole	Sample depth (m)	Lithology	Alteration zone	LOI (%)[a]	δ18O ‰ VSMOW	±2σ	87Sr/86Sr	±2σ	Sr (mg/kg)[a]	Rb (mg/kg)[a]	% Sr exchange	W/R (Sr)	W/R (δ18O) δw = 0.2	W/R (δ18O) δw = −3.5	W/R (δ18O) δw = −8.03	W/R (δ18O) δw = −12
RN-17	350	Basaltic tuff	Epidote–MLC	4.46	3.25	0.60	0.704378	±0.000011	177.3	16.7	19.76	4.1	1.6	0.5	0.3	0.2
	400	Claystone	Epidote–MLC	4.38	1.89	0.60	0.704911	±0.000009	114.4	13.0	28.71	6.0	20.8	1.0	0.5	0.3
	500	Basaltic breccia	Epidote–MLC	3.26	1.50	0.60	0.703798	±0.000011	198.4	0.0	10.04	2.1	−21.7	1.2	0.5	0.4
	550	Sedimentary tuff	Chlorite–epidote	3.00	1.48	0.60	0.703971	±0.000009	160.8	0.1	12.94	2.7	−19.8	1.2	0.5	0.4
	600	Sedimentary tuff	Chlorite–epidote	4.14	1.48	0.60	0.704256	±0.000011	177.3	1.2	17.72	3.7	−19.7	1.2	0.5	0.4
	650	Sedimentary tuff	Chlorite–epidote	4.94	3.61	0.60	0.704675	±0.000014	158.1	7.6	24.75	5.2	1.1	0.4	0.2	0.2
	700	Sedimentary tuff	Chlorite–epidote	–	–	–	0.704720	±0.000013	137.2	2.9	25.51	5.3				
	750	Basaltic breccia	Chlorite–epidote	2.84	0.85	0.60	0.704098	±0.000015	148.8	0.9	15.07	3.1	−5.8	1.7	0.7	0.4
	800	Basaltic breccia	Chlorite–epidote	3.66	1.42	0.60	0.703835	±0.000011	159.9	0.3	10.66	2.2	−15.6	1.3	0.6	0.4
	800	Basaltic breccia	Chlorite–epidote	3.66	1.58	0.60	–	–	–	–	–		−35.3	1.2	0.5	0.3
	850	Sedimentary tuff	Chlorite–epidote	3.18	1.59	0.60	0.704181	±0.000012	109.8	1.7	16.46	3.4	−38.3	1.2	0.5	0.3
	1000	Basaltic breccia	Chlorite–epidote	2.65	2.67	0.60	0.706098	±0.000017	229.8	2.8	48.63	10.2	3.2	0.7	0.3	0.2
	1050	Glassy basalt	Chlorite–epidote	2.03	1.73	0.60	0.704162	±0.000019	82.8	1.0	16.14	3.4	122.0	1.1	0.5	0.3
	1150	Medium-coarse crystalline basalt	Chlorite–epidote	2.12	2.72	0.60	0.703743	±0.000016	148.4	0.0	9.11	1.9	3.0	0.7	0.3	0.2
	1200	Glassy basalt	Epidote–actinolite	1.86	2.09	0.60	0.703648	±0.000010	132.2	0.9	7.52	1.6	9.4	0.9	0.4	0.3
	1350	Glassy basalt	Epidote–actinolite	2.64	1.89	0.60	0.705216	±0.000012	184.0	0.0	33.82	7.1	20.5	1.0	0.5	0.3
	1400	Medium-coarse crystalline basalt	Epidote–actinolite	2.35	1.46	0.60	0.703754	±0.000014	151.0	0.3	9.30	1.9	−18.0	1.3	0.5	0.4
	1500	Medium coarse crystalline basalt	Epidote–actinolite	0.79	1.46	0.60	0.703338	±0.000016	151.1	3.1	2.32	0.5	−17.8	1.3	0.5	0.4
	1550	Fine-medium crystalline basalt	Epidote–actinolite	0.74	1.11	0.60	0.703335	±0.000016	155.9	4.2	2.27	0.5	−8.0	1.5	0.6	0.4
	1650	Fine-medium crystalline basalt	Epidote–actinolite	0.68	1.84	0.60	0.703306	±0.000011	144.2	6.2	1.78	0.4	28.6	1.0	0.5	0.3
	1750	Basaltic tuff	Epidote-actinolite	2.54	−0.05	0.60	0.703929	±0.000014	137.4	0.0	12.23	2.6	−3.3	3.0	0.9	0.6
	1800	Basaltic tuff	Epidote-actinolite	2.41	−0.13	0.60	0.704542	±0.000016	124.3	8.2	22.51	4.7	−3.2	3.2	0.9	0.6
	1850	Basaltic tuff	Epidote-actinolite	2.95	1.00	0.60	0.703712	±0.000016	151.8	0.1	8.59	1.8	−6.8	1.6	0.6	0.4
	1950	Coarse crystalline basalt	Epidote-actinolite	1.54	1.11	0.60	0.703569	±0.000013	105.2	0.0	6.19	1.3	−7.9	1.5	0.6	0.4
	2000	Coarse crystalline basalt	Epidote-actinolite	1.29	2.44	0.60	0.703374	±0.000021	166.0	0.8	2.91	0.6	4.5	0.8	0.4	0.3
	2150	Coarse crystalline basalt	Epidote-actinolite	1.24	2.07	0.60	0.703378	±0.000013	156.5	1.3	2.99	0.6	10.2	0.9	0.4	0.3
	2300	Basaltic breccia	Epidote-actinolite	1.86	0.99	0.60	0.703795	±0.000012	126.2	0.0	9.98	2.1	−6.8	1.6	0.6	0.4
	2350	Basaltic breccia	Amphibole	1.20	1.19	0.60	0.703881	±0.000013	114.8	0.0	11.42	2.4	−9.1	1.4	0.6	0.4
	2500	Coarse crystalline basalt	Amphibole	1.88	2.15	0.60	0.704454	±0.000014	149.9	0.0	21.04	4.4	8.2	0.9	0.4	0.3
	2500	Coarse crystalline basalt	Amphibole	1.88	2.37	0.60	–	–	–	–	–		5.1	0.8	0.4	0.3
	2650	Glassy basalt	Amphibole	1.68	1.56	0.60	0.703733	±0.000015	134.0	0.3	8.94	1.9	−31.3	1.2	0.5	0.4
	2800	Coarse crystalline basalt	Amphibole	1.08	2.27	0.60	0.703289	±0.000013	143.7	2.0	1.49	0.3	6.2	0.8	0.4	0.3
	2900	Glassy basalt	Amphibole	1.22	1.33	0.60	0.703573	±0.000015	135.8	0.0	6.25	1.3	−12.2	1.3	0.6	0.4
	3000	Glassy basalt	Amphibole	1.72	0.78	0.60	0.703746	±0.000026	157.7	0.0	9.16	1.9	−5.4	1.8	0.7	0.4
	3050	Glassy basalt	Amphibole	1.36	1.18	0.60	0.703546	±0.000013	125.4	0.0	5.81	1.2	−9.0	1.4	0.6	0.4
RN-17B	2804.5	Volcanic sediment	Amphibole	–	0.97	0.60	0.703907	±0.000016	–	–	11.87	2.5	−6.7	1.6	0.6	0.4
	2804.8	Breccia w/ hyaloclastite matrix and light colored alteration	Amphibole	–	0.90	0.60	0.703907	±0.000011	–	–	11.86	2.5	−6.1	1.7	0.7	0.4
	2802.9	Heterolithic breccia w/ hyaloclastite matrix	Amphibole	–	0.62	0.60	0.703968	±0.000018	–	–	12.89	2.7	−4.8	2.0	0.7	0.5
	Mean values			2.3	1.58		0.703992				13.3	2.8			0.5	0.4

[a] Loss on Ignition (LOI%), Rb (mg/kg), Sr (mg/kg) are from Marks et al., 2010.
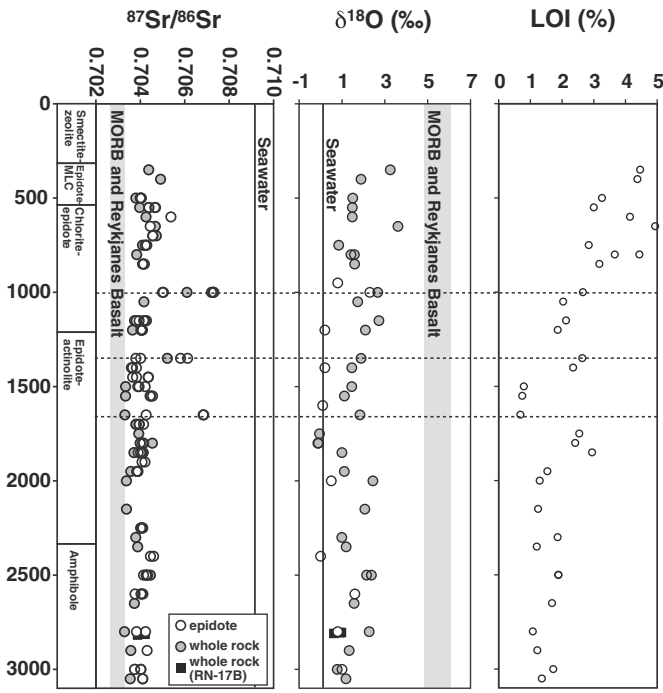
Fig. 5. Strontium and oxygen isotope and Loss on Ignition (LOI) profiles for whole rock cuttings, core, and epidote for well RN-17 and RN-17B core. Epidote oxygen isotope data are from Pope et al., 2009. LOI data are from Marks et al., 2010. Dashed lines indicate inferred feed zones.

A simple closed-system mass balance equation for water/rock ratio derived from oxygen isotopes was proposed by Taylor (1974):

$$W/R\,(^{18}O) = (\delta_{AR} - \delta_{FR})/(\delta_W - (\delta_{AR} - \Delta))$$

where δ_{AR} is the oxygen isotopic value of altered rock, δ_{FR} is the isotopic value of fresh rock, and δ_W is the isotopic value of the initial fluid. As stated in Alt and Teagle (2000), interpretation of water/rock ratios based on oxygen isotope values of whole rocks can be problematic

when applied to oceanic crust and ophiolites due to violation of the assumptions of the method, including complete recrystallization and attainment of isotopic equilibrium. It has however been widely applied (Spooner et al., 1977; Gregory and Taylor, 1981; Alt et al., 1986; Harper et al., 1988) to ophiolites and oceanic crust in an attempt to constrain hydrothermal flux. Applying the approach to the Reykjanes rocks is, however, somewhat problematic. Choosing a value for δ_{FR} is relatively straight forward, though a range of isotopic values has been reported for unaltered basalts of the Reykjanes peninsula, ($\delta^{18}O = 5.0$–$6.3‰$; Hemond et al., 1988). A nominal value of $\delta_{FR} = 5.8‰$, typical of oceanic basalts was used in the calculations. The oxygen isotope water-rock fractionation factor Δ is defined as $\Delta = \delta_{AR} - \delta_{HF}$, the difference between the altered rock and the hydrothermal fluid. For equilibrium exchange, Δ is dependent on temperature ($\Delta \propto 1/T^2$) with a decreasing value at increased temperature. Taylor (1974) made the assumption that Δ for many hydrothermal systems hosted in igneous rock could be approximated by temperature dependent water-plagioclase exchange using an An_{30} as a representative value altered rock. The Reykjanes geothermal system is a mature geothermal upflow zone, with a shallow temperature gradient (Fig. 3). The bulk of the greenschist-altered samples analyzed were sampled at in situ temperatures that ranged from 280 °C to 320 °C. Using Taylor's approach, Δ should vary from 5.2‰ at 280 °C to 4.1‰ at 320 °C, with a value of 4.6‰ at 300 °C, a reasonable average temperature for the greenschist-altered rocks at the depths analyzed in this study.

We used an alternative approach to calculate Δ based on modal abundance of alteration minerals. The cuttings analyzed are dominantly greenschist-facies altered basalt with approximate modal abundance of alteration phases of chlorite (~15%), An_{30} plagioclase (~35%), epidote (~10%), actinolite (~40%). We assumed isothermal fractionation to be occurring at ~300 °C throughout the hole, and calculated a normalized fractionation factor of $\Delta = 1.7‰$ for the altered portions of the rock based on the modal of abundance the above minerals and the fractionation curves for each of these minerals generated by Matsuhisa et al. (1979) and Cole and Ripley (1999). The lower value for Δ results from the lower degree of fractionation for chlorite and actinolite relative to An_{30} plagioclase. We estimate the general extent of alteration as ~35%, which results in a whole-rock Δ value of 4.4‰; nearly identical to the 4.6‰ value calculated by Taylor's method. The similarity of alteration

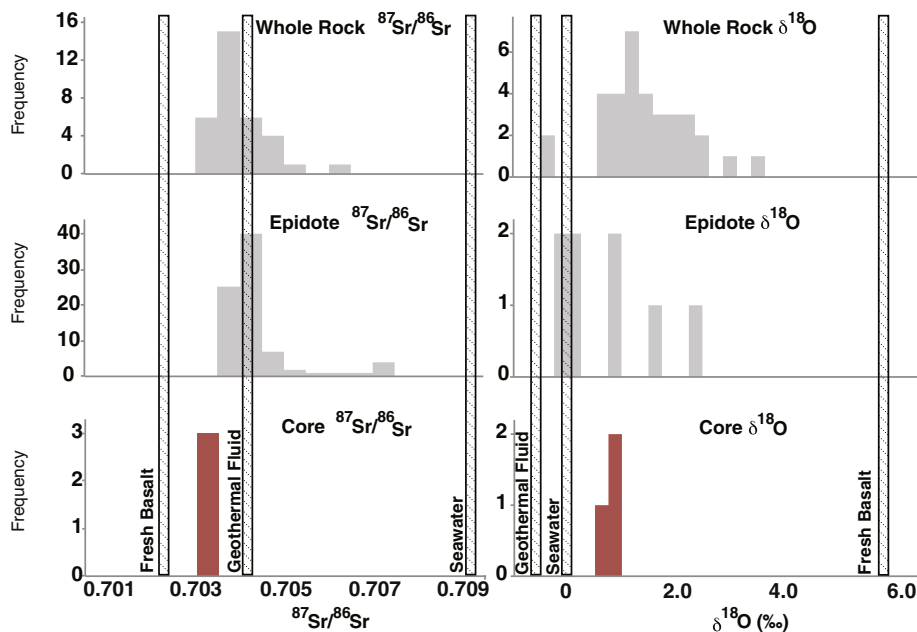**Fig. 6.** Histograms showing distribution of measured $^{87}Sr/^{86}Sr$ and d18O isotopic values measured in the whole rock cuttings, epidotes, and core samples relative to seawater, local geothermal fluids and primary magmatic values.
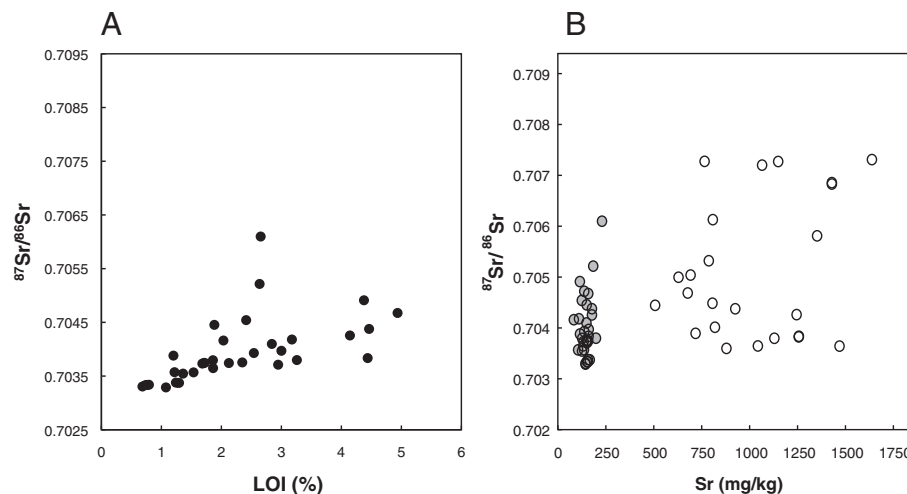
Fig. 7. A) Plot of whole rock $^{87}Sr/^{87}Sr$ ratios vs. LOI. Fresh Reykjanes basalts typically have LOI in the range of 0.5 wt.%, values above 1 wt.% indicate significant hydrous secondary mineralization. B) $^{87}Sr/^{87}Sr$ ratios versus Sr concentration for whole rock samples (shaded symbols) and epidote (open symbols).

mineralogy observed in the mid-crustal sections of altered oceanic crust and ophiolites to that observed in the Reykjanes rocks suggests that assuming a value of $\Delta = 4.4‰$ is appropriate.

Calculation of water rock ratios requires knowledge of the isotopic value of the fluid prior to interaction with the rock, which is more problematic. Water/rock calculations for altered oceanic crust or ophiolites generally assume a value near present day seawater (0‰). This appears to be a reasonable choice for the Reykjanes system, as the present day hydrothermal fluid in the Reykjanes geothermal system has the chemical and isotope composition of evolved seawater (Sveinbjornsdottir et al., 1986; Arnórsson, 1995; Pope et al., 2009). Assuming an initial water isotopic value of 0‰ results in calculated water/rock ratios that are negative, a meaningless result. Varying the choice of Δ about any reasonable value related to the temperature of alteration does not change this result. Equilibrium exchange between water and rock composed of the observed alteration minerals always results in the altered rock having higher $\delta^{18}O$ values than the water with which it equilibrates. Assuming a kinetic isotope effect where the mineral bonds to the lighter isotope are preferentially broken make the situation even worse. The low $\delta^{18}O$ values measured on the altered basaltic rocks at Reykjanes can only be reconciled by assuming the altering fluid had a value lighter than seawater. Variable salinity in fluid inclusions hosted in hydrothermal alteration minerals (Franzson et al., 2002) and low δD values of hydrothermal alteration minerals (Pope et al., 2009) suggest that meteoric waters, which would be depleted in $\delta^{18}O$ relative to seawater, have been involved at an earlier stage of hydrothermal alteration in the Reykjanes system. Present day meteoric water in the area has a $\delta^{18}O$ value of approximately $-8‰$ (IAEA WISER database, 345 samples collected monthly between 1960 and 2009). If significant alteration occurred during the last glacial maximum, the locally sourced meteoric water would be expected to have even lower $\delta^{18}O$, perhaps as low as $-12‰$ (i.e. Dansgaard, 1964).

Pope et al. (2009) also concluded that epidotes with $\delta^{18}O$ less than $-0.1‰$ could not have formed in equilibrium with seawater or present-day geothermal fluids. Present day hydrothermal fluids from deep wells at Reykjanes (>2000 m) have average $\delta^{18}O$ values of $-0.6‰$ and δD of $-20.8‰$ (Pope et al., 2009), with a range of $\delta^{18}O$ from 2.3‰ to $-1.1‰$ (Árnason, 1977; Ólafsson and Riley, 1978; Pope et al., 2009). The hydrogen isotope values of epidotes also do not appear to be in equilibrium with present day hydrothermal fluid. Pope et al. (2009) used mass balance at an assumed water/rock ratio of 0.25, similar to that posited by Cole et al. (1998) based on $\delta^{18}O$ data from

Sveinbjornsdottir et al. (1986), to argue that δD of epidote and δD of present day hydrothermal fluid is the result of diffusional exchange between the modern-day seawater-derived geothermal system and hydrothermally altered rocks with bulk-rock $\delta^{18}O = -5.9‰$ and $\delta D = -125‰$ formed during an earlier period when the Reykjanes system was recharged by glacially derived fluids.

Water-rock ratios presented in Table 1 were calculated assuming that the initial fluids had $\delta^{18}O = -5.9‰$, following Pope et al., 2009, which is consistent with an integrated water rock alteration regime that evolved from meteoric water to sea water as the dominant source of recharge fluids. Sveinbjornsdottir et al. (1986) proposed that geothermal fluids have evolved from a meteoric dominated to seawater-dominated source based on oxygen isotope analyses of quartz. The calculated water/rock values range from 0.5 to 2.2, with the exception of two highly altered samples of basaltic tuff that range up to 4.3. These values overlap the range of values calculated for oceanic crust and ophiolites (e.g. Spooner et al., 1977; Gregory and Taylor, 1981; Michard et al., 1984.), although somewhat higher than estimates for fast spreading oceanic crust (i.e. Mottl, 1983). This observation is not surprising considering that the Reykjanes rocks are typically more vesicular and have greater permeability than submarine rocks, particularly gabbros. In addition, the vigorous hydrothermal circulation characteristic of the Reykjanes system would be expected to result in greater alteration and isotopic exchange than in a submarine setting. Variation in water/rock ratios is weakly correlated with rock type; more porous and reactive lithologies (i.e. tuffs and breccias) have somewhat higher calculated water/rock ratios than crystalline basalts. There is also a slight increase in water/rock ratio with depth; this could reflect lithologic changes in the samples, although there is no correlation with LOI or other indicators of alteration. There is no observable increase in water/rock ratio at known feed zones, perhaps indicating that these are new feed zones that have not yet had time to equilibrate with the hydrothermal fluid.

Assuming that all the alteration was due to interaction with local meteoric water with $\delta^{18}O = -8‰$ results in lower water/rock ratios (0.3–1.7), but as discussed below, this assumption is at odds with the Sr isotope profile measured on the samples.

5.2. Strontium isotopes

Strontium is a useful tracer for seawater–crustal interactions because the $^{87}Sr/^{86}Sr$ ratios of seawater (0.70916) and fresh Reykjanes

Table 2
Oxygen and strontium isotope compositions in epidote grains from RN-17.

Sample ID	Depth (m)	Grain	Location	$^{87}Sr/^{86}Sr$	$\pm 2\sigma$	$\delta^{18}O$ Average[a]	Sr (mg/kg)
500m_Line2	500	1	Rim	0.70405	± 0.00013		
500m_Line1	500	1	Core	0.70399	± 0.00014		
500mLine3	500	1	Rim	0.70402	± 0.00019		
550mSpot1	550	1	Core	0.70439	± 0.00007		925
550mSpot2	550	1	Rim	0.70465	± 0.00008		
550mLine1	550	2	Rim	0.70469	± 0.00013		677
600mLine1	600	1	Core	0.70538	± 0.00017		
650mLine1	650	1	Core	0.70445	± 0.00020		507
700mSpot1	700	1	Core	0.70457	± 0.00004		
700mSpot2	700	2	Core	0.70456	± 0.00007		
750mSpot1	750	1	Core	0.70424	± 0.00009		
750mSpot3	750	2	Core	0.70422	± 0.00009		
750mSpot2	750	3	Core	0.70429	± 0.00014		
850mLine1	850	1	Core	0.70410	± 0.00005		
850mLine2	850	1	Rim	0.70415	± 0.00007		
1000m_Spot1	1000	1	Core	0.70500	± 0.00015		629
1000m_Line2	1000	2	Core	0.70504	± 0.00018	2.3	692
1000m_Line3	1000	2	Rim	0.70731	± 0.00016		1638
1000m_Line4	1000	2	Rim	0.70727	± 0.00009		1149
1000m_Line5	1000	2	Rim	0.70728	± 0.00016		765
1000m_Line6	1000	2	Rim	0.70720	± 0.00010		1065
1150m_Line1	1150	1	Core	0.70382	± 0.00019		
1150m_Line4	1150	1	Core	0.70395	± 0.00010		
1150m_Line5	1150	1	Rim	0.70415	± 0.00016		
1200mLine1	1200	1	Rim	0.70404	± 0.00006	0.2	
1200mLine2	1200	1	Rim	0.70409	± 0.00005		
1200mLine3	1200	1	Core	0.70403	± 0.00009		
1200mLine4	1200	1	Core	0.70409	± 0.00004		
1200mLine5	1200	1	Rim	0.70405	± 0.00007		
1350mLine1	1350	1	Rim	0.70581	± 0.00010		1352
1350mLine2	1350	1	Core	0.70613	± 0.00008		808
1350mLine3	1350	1	Transition	0.70401	± 0.00009		819
1350mLine4	1350	1	Rim	0.70380	± 0.00009		1129
1400mSpot1	1400	1	Core	0.70365	± 0.00006		1043
1400mLine1	1400	2	Rim	0.70364	± 0.00007	0.2	1469
1400mLine2	1400	2	Transition	0.70382	± 0.00007		1256
1400mLine3	1400	2	Core	0.70360	± 0.00008		879
1450mLine1	1450	1	Rim	0.70437	± 0.00008		
1450mLine2	1450	1	Rim	0.70435	± 0.00010		
1450mLine3	1450	1	transition	0.70383	± 0.00015		
1450mLine4	1450	1	Core	0.70366	± 0.00013		
1500mLine1	1500	1	Core	0.70394	± 0.00011		
1500mLine2	1500	1	Transition	0.70388	± 0.00011		
1500mLine3	1500	1	Rim	0.70422	± 0.00018		
1550mSpot1	1550	1	Core	0.70455	± 0.00009		
1550mLine1	1550	2	Core	0.70444	± 0.00012		
1550mSpot2	1550	3	Core	0.70447	± 0.00013		
1650mLine-4	1650	1	Core	0.70426	± 0.00016		1245
1650mLine-1	1650	1	Rim	70.70683	± 0.00019		1429
1700mLine1	1700	1	Core	0.70396	± 0.00008		
1700mLine2	1700	1	Core	0.70380	± 0.00014		
1700mLine3	1700	1	Transition	0.70394	± 0.00011		
1700mLine4	1700	1	Rim	0.70415	± 0.00011		
1700mLine5	1700	1	rim	0.70382	± 0.00014		
1800mSpot1	1800	1	Core	0.70415	± 0.00007	−0.1	
1800mLine2	1800	2	Core	0.70399	± 0.00010		
1800mSpot2	1800	3	Core	0.70400	± 0.00011		
1850mLine3	1850	1	Core	0.70390	± 0.00019		
1850mLine2	1850	1	Rim	0.70412	± 0.00020		
1900mSpot1	1900	1	Core	0.70408	± 0.00010		
1900mLine1	1900	2	Core	0.70421	± 0.00012		
1950mSpot2	1950	1	Core	0.70384	± 0.00007		1257
1950mLine1	1950	2	Core	0.70387	± 0.00014		
1950mSpot1	1950	3	Core	0.70389	± 0.00014		718
2250mLine3	2250	1	Rim	0.70402	± 0.00015		
2250mLine2	2250	1	Rim	0.70403	± 0.00016		
2400mLine2	2400	1	Core	0.70446	± 0.00015		
2400mLine1	2400	1	Rim	0.70460	± 0.00015	0	
2500mLine1	2500	1	Rim	0.70428	± 0.00018		
2500mLine2	2500	1	Core	0.70415	± 0.00020		
2500mLine3	2500	1	Rim	0.70426	± 0.00015		
2600mLine2	2600	1	Core	0.70376	± 0.00015		
2600mLine3	2600	1	Rim	0.70405	± 0.00019	1.6	
2600mLine4	2600	1	Rim	0.70403	± 0.00019		
2800mLine1	2800	1	Core	0.70383	± 0.00015	0.8	

Table 2 (continued)

Sample ID	Depth (m)	Grain	Location	$^{87}Sr/^{86}Sr$	$\pm 2\sigma$	$\delta^{18}O$ Average[a]	Sr (mg/kg)
2800mLine2	2800	1	Rim	0.70424	± 0.00019		
2900mLine1	2900	1	Core	0.70430	± 0.00019		
3000mLine2	3000	1	Rim	0.70403	± 0.00015		
3000mLine4	3000	1	Core	0.70374	± 0.00019	1	
3050mLine2	3050	1	Core	0.70411	± 0.00017		
3050mLine1	3050	1	Core	0.70411	± 0.00018		
Mean epidote value				0.70437			

[a] Oxygen data from Pope et al., 2009.

basalt (0.70320) are significantly different and there is no temperature- or mineral-dependent isotopic fractionation of strontium. Strontium isotope ratios of altered rocks, minerals, and fluids can therefore provide a measure of the interaction of seawater with oceanic crust. The degree of Sr isotopic exchange is given by:

$$\% \text{ SW Exchange} = \left(^{87}Sr/^{86}Sr\right)_{AR} - \left(^{87}Sr/^{86}Sr\right)_{FR}$$
$$/ \left(^{87}Sr/^{86}Sr\right)_{SW} - \left(^{87}Sr/^{86}Sr\right)_{FR} * 100$$

where the subscripts refer to the following: AR = altered rock; FR = Fresh rock; SW = seawater (Davis et al., 2003). This calculation assumes the starting fluid is not affected by any admixed meteoric water, a reasonable assumption given that precipitation typically has a concentrations of ~2–200 ppb Sr (Bacon and Bain, 1995; Graustein and Armstrong, 1983). Samples from RN-17 show a range of isotopic exchange from ~1.5 to 49% exchange, with a mean value of 13% (Table 1). The two most exchanged samples (at 1000 and 1350 m) correspond to hydrothermal feed points or lithological transitions (Fig. 7). Hyaloclastite, breccia, and tuff samples have the highest exchange, typically 11–20%. Less reactive crystalline basalts typically have exchange ratios of less than 5%. These values are comparable to exchange ratios calculated for oceanic crust (i.e. ODP Hole 504B, 5–12%; ODP Hole 417D and 418A ~19%; Davis et al., 2003).

We also measured strontium isotopes in epidote as the $^{87}Sr/^{86}Sr$ is largely interpreted to be representative of the fluid from which epidote precipitated (Bird and Spieler, 2004; Gillis et al., 2005). The epidote spot analyses range from 0.70360 to 0.70731, with a mean composition of 0.70437. This mean value is, in fact, quite similar to the present-day strontium isotope composition of geothermal fluids from the Reykjanes Geothermal system (0.70412–0.70421; Elderfield and Greaves, 1981; Millot et al., 2009). Epidote with higher $^{87}Sr/^{86}Sr$ (>0.704) is attributed to larger amounts of seawater reacting with the Reykjanes basalt, which may reflect local variations in permeability, fluid pathways, and mixing of fluids within the subsurface. Precipitation of Sr-bearing alteration phases (i.e. calcite, anhydrite) in the recharge limb of the hydrothermal circulation cell can also influence the strontium isotope ratio of the hydrothermal fluid. The greatest differences in $^{87}Sr/^{86}Sr$ in bulk cuttings compared to epidote occurs in samples located proximal to feed zones, presumably because it is at these feed zones where fresher fluids that are less exchanged with the basalts are entering the system.

We also calculate W/R ratios for seawater exchange based on whole rock $^{87}Sr/^{86}Sr$ measurements using the following equation, adapted from McCulloch et al. (1980):

$$W/R_{Sr} = Sr_{FR}/Sr_{SW} * \left(\left(^{87}Sr/^{87}Sr_{AR}\right) - \left(^{87}Sr/^{87}Sr_{FR}\right)\right)$$
$$/ \left(\left(^{87}Sr/^{87}Sr_{SW}\right) - \left(^{87}Sr/^{87}Sr_{FR}\right)\right)$$

where Sr_{FR} is the concentration of Sr in fresh rock (~167 mg/kg), Sr_{SW} is the concentration of strontium in seawater (8 mg/kg), $^{87}Sr/^{87}Sr_{AR}$ is the isotope composition of altered rock, $^{87}Sr/^{87}Sr_{FR}$ is the isotope composition of fresh rock at Reykjanes (0.70320), and $^{87}Sr/^{87}Sr_{SW}$ is the isotope composition of seawater (0.70916). The ratios obtained range from 0.3 to 10.2 (mean 2.8) and generally decrease with depth. The highest values occur in the previously noted zones at 1000 and 1350 m (Fig. 8). Variation in the water/rock ratios calculated corresponds to different rock types; crystalline basalts have lower water/rock ratios (typically <2) than more porous and reactive hyaloclastite and brecciated samples (typically 2–6). The decreasing water/rock ratios with depth most likely reflect the permeability structure of the Reykjanes system, with the more permeable hyaloclastites, which generally occur within the upper 1000 m of RN-17, having the highest $^{87}Sr/^{86}Sr$ ratios.

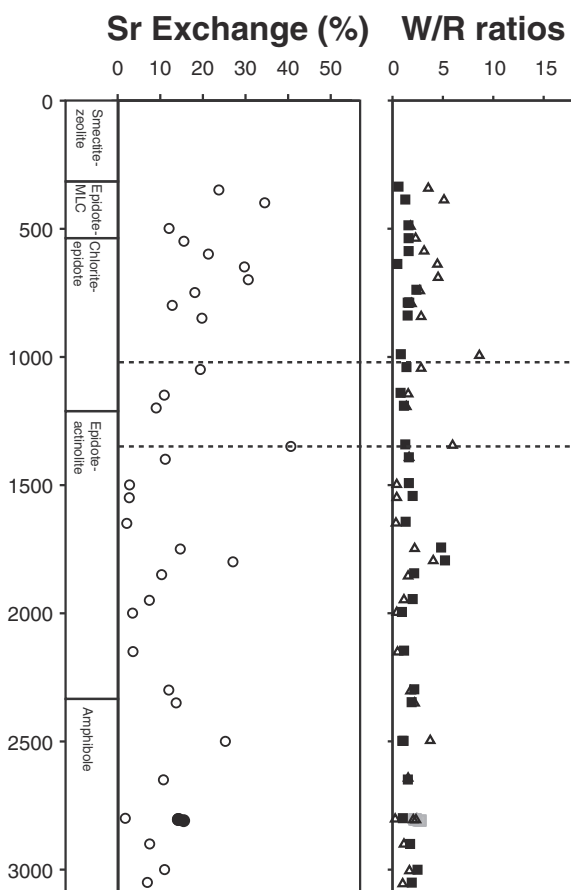**Sr Exchange (%)   W/R ratios**

Fig. 8. Percent exchange with seawater Sr and water/rock ratio profiles for whole rock samples from RN-17 cuttings and RN-17B core, calculated as discussed in text. In the first panel, open symbols are calculated based on cuttings, black symbols are from core. In the second panel, the black squares indicate water/rock ratios calculated from $^{87}Sr/^{86}Sr$ measurements on cuttings, gray squares are based on core, and open triangles are calculated from $\delta^{18}O$ measurements. Dashed lines indicate inferred feed zones.

5.3. Comparison of Sr and $\delta^{18}O$

Water/rock ratios calculated from Sr and $\delta^{18}O$ isotopic systems are qualitatively similar, except for the complications of temperature-sensitive mineral-fluid fractionations. Ratios based on strontium isotopes tend to be somewhat higher (0.3–10, mean 2.8) than those based on oxygen isotopes (0.4–4.3, mean 1.6). The Sr isotopic system clearly indicates extensive exchange with seawater, whereas the oxygen isotopic system is more sensitive to exchange with a meteoric-derived fluid. The combined use of $^{87}Sr/^{86}Sr$ and $\delta^{18}O$ confirms contributions of each of the proposed end-member fluids in alteration.

One additional clue to the early history of the Reykjanes system is the observation of isotopic zoning within a number of individual epidote grains. Many epidote cores contain less radiogenic Sr than the rims of the crystals, which suggests an increasing influence of seawater dominated fluids through time. Strontium isotope compositions of epidotes from the same depth can show a wide compositional range with differences between $^{87}Sr/^{87}Sr$ in most and least radiogenic epidote ranging up to 0.003. Since strontium isotopes are not fractionated during epidote precipitation, these differences must reflect variation in the composition of the geothermal fluid (Alt et al., 1996; Bird and Spieler, 2004). Further study of oxygen isotopic zonation across epidote grains could confirm the importance of meteoric fluids in the early mineralization of the Reykjanes system. The alteration minerals expected to precipitate from saline fluids are very similar to those expected to precipitate from meteoric-water dominated fluids, therefore the cuttings and core lack a distinctive mineralogical expression of this early meteoric stage of alteration. The mineralogical data therefore do not contradict interpretations based on isotopic and fluid inclusion evidence that the Reykjanes geothermal system was meteoric-water dominated in its early history (Franzson et al., 2002; Pope et al., 2009; this study). This implies that the Reykjanes system has been active for an extended time, likely since the last glacial maximum (Franzson et al., 2002; Marks et al., 2010) Petrographic evidence from the RN-17B core and RN-17 cuttings indicates multiple episodes of hydrothermal alteration within the system, including cross cutting veins and replacement of amygdale fillings. Mineral assemblages ranging from greenschist to amphibolite to pyroxene hornfels facies have been observed in metastable alteration patches suggesting local equilibration within different areas of the system, and shallow high-temperature assemblages suggest temporal variability in pressure and temperature. The observed metastable assemblages suggest different stages of hydrothermal alteration, each with distinct hydrothermal fluids.

The general trend of increasing $^{87}Sr/^{86}Sr$ with decreasing $\delta^{18}O$ in the intrusive section of the hole below 1350 m appears to reflect varying extents of recrystallization in the intrusive suite. The positive correlation of $^{87}Sr/^{86}Sr$ with LOI (Fig. 7) may reflect an overall increase in the abundance of hydrous phases (e.g. Alt et al., 1996; Kirchner and Gillis, 2012). Core samples appear to be more altered than cuttings, with slightly higher $^{87}Sr/^{86}Sr$ ratios and lower $\delta^{18}O$ ratios than whole rock cutting samples with similar lithology, which suggests that preferential recovery of less altered material in cuttings may slightly bias estimates of isotopic exchange.

5.4. Comparison of RN-17 and analogous submarine systems

The Reykjanes geothermal system bears a number of similarities to mid-ocean ridge hydrothermal systems in terms of the alteration mineralogy and geochemistry of the hydrothermal fluids and the sulfide minerals precipitated from those fluids (Hardardóttir et al., 2009, 2010). High-temperature hydrothermal systems at slow and fast spreading ridges are characterized by several important differences that have bearing on this current work (i.e. German and Lin, 2004). Fast and intermediate spreading ridges are supplied by significantly greater magmatic heat fluxes than slower spreading ridges, and are typified by hydrothermal venting activity that is in response to episodic

magmatic heat release (German and Lin, 2004). In contrast, vent fields along slow spreading ridge sections such as the Mid Atlantic Ridge are typically larger, more widely spaced and longer lasting than those observed in the Pacific. It has been suggested that the energy for these systems includes components of heating from the crystallization of basaltic magma, cooling of solidified gabbro and basalt from >1000° to hydrothermal temperatures of ~350°, as well as a component of energy from the latent heat of serpentinization of ultramafic rocks (German and Lin, 2004). Some of the large submarine systems show evidence of interaction with serpentinizing ultramafic rocks (Charlou et al., 2002; Douville et al., 2002). For example at the TAG field and elsewhere, faulting has apparently shifted the pathways of hydrothermal fluid flow over long time scales to extract heat from the crust–mantle boundary over long timescales (Canales et al., 2007; deMartin et al., 2007). In contrast, the geothermal system at Reykjanes lacks evidence of interaction with ultramafic rocks, which is unsurprising given the thickness of the Icleandic basaltic plateau. Further, the heating regime for the Reykjanes system, which involves excess volcanism due to the increased temperature of Iceland mantle plume might suggest that the thermal regime is similar to fast or intermediate spreading hydrothermal analogs, despite the slow extension rate. The size of the Reykjanes system (130 ± 16 MW; Fridriksson et al., 2006) is also more similar to the smaller systems associated with fast and intermediate spreading ridges than the massive systems associated with the MAR (i.e. the mafic intrusion driven Rainbow Hydrothermal Field 2.3 GW; Thurnherr and Richards, 2001). For these reasons we have chosen to focus on comparisons of hydrothermal systems from fast spreading ridges rather than slow spreading ridges.

Similar to the results from Reykjanes, bulk-rock $^{87}Sr/^{86}Sr$ ratios from altered, in-situ oceanic crust are typically shifted away from MORB values (~0.7027; Salters and Stracke, 2004) towards seawater values (0.70916; Palmer and Edmond, 1989). The isotope ratios of in-situ crust sampled in ODP Hole 504B generally range from 0.70265–0.70304, with some chlorite and amphibole veins up to 0.7038 (Kawahata et al., 1987; Alt et al., 1996). Bulk rock values for IODP Hole 1256D basalts are similar throughout much of the hole (0.7028–0.7038) with rare patches of enhanced alteration adjacent to lithological transitions that have far more radiogenic values up to 0.7075 (Harris et al., 2015). Typical hydrothermal vent fluids have a more radiogenic Sr isotope composition (~0.7037–0.70465; Palmer and Edmond, 1989; Bach and Humphris, 1999; Ravizza et al., 2001) indicating increased seawater input relative to the fluids that circulated through the crust at 1256D. These ratios are higher than estimates from ODP Hole 504B but are consistent with values inferred from vent fluids from 21° and 13°N on the East Pacific Rise (Albarède et al., 1981). The whole rock Sr isotope profile though IODP Hole 1256D shows limited increases in $^{87}Sr/^{86}Sr$ in the volcanic sequence, however higher $^{87}Sr/^{86}Sr$ zones provide evidence for channelized flow (and thus greater isotopic exchange) at the top of massive flow sequences, at the lava–dike transition, and along dike margins (Harris et al., 2015). The model of channelized hydrothermal fluid flow invoked by Harris et al. (2015) explains the dramatic contrast in $^{87}Sr/^{86}Sr$ between the massive basalt flows and dike cores and the far more altered high $^{87}Sr/^{86}Sr$ horizons in IODP Hole 1256D. Since the Reykjanes geothermal system is a zone of focused hydrothermal upflow, similar to the zones of channelized flow in MOR settings, the more radiogenic Sr signal appears to reflect the enhanced interaction of the host rocks along the hydrothermal discharge pathway.

6. Conclusions

Rocks from the Reykjanes geothermal system have been extensively altered by interaction with both meteoric water and seawater, in a long lived, evolving hydrothermal system that appears to have been active beneath an ice cover during the last glacial maximum. Strontium isotope compositions of altered rocks and the present day geothermal

fluids are significantly shifted towards seawater values. Oxygen isotopes in whole rock samples are also shifted away from basaltic values, and indicate the importance of a meteoric-derived hydrothermal fluid earlier in the alteration history of this geothermal system.

Calculations of fluid/rock ratios based on isotopic indicators of exchange have customarily been made with an equilibrium model based on two critical assumptions (e.g. Taylor, 1974; Taylor, 1979; Forester and Taylor, 1980). The first is that rock and fluid readily attain isotopic equilibrium at some specific temperature below which no further isotopic exchange can occur. The second is that the equilibrium isotopic fractionation factors between rock and fluid can be closely approximated by those for particular mineral-water systems (i.e. An30 plagioclase-water for the oxygen system). Although this approach has been useful, there are a number of limitations to the method that must be considered. One limitation is that rock and fluid in many geothermal systems may not be in isotopic equilibrium; some systems show evidence of disequilibrium at temperatures in excess of 300 °C, while in other systems equilibration appears complete at temperatures below 120 °C (e.g. Casadevall and Ohmoto, 1977; Cole, 1983; Green et al., 1983). Regions of a geothermal system may be heterogeneously equilibrated. Finally, in an evolving system like Reykjanes, fluids may pass through previously altered rock that has equilibrated with a different fluid. Given the limitations of water/rock ratio calculations, particularly in a system with variable thermal conditions and fluid compositions, it is remarkable that the calculated values so closely resemble the characteristics of submarine hydrothermal systems with presumably more stable fluid compositions. The similarities in water/rock ratio are perhaps even more remarkable in light of the dramatically different crustal thicknesses and depth to heat sources between Mid-Ocean Ridge systems and Reykjanes. Although the particulars differ, the basic controls on fluid–rock interaction at Reykjanes appear to be quite similar to submarine hydrothermal systems.

Acknowledgments

References

Albarède, F., Michard, A., Minster, J., Michard, G., 1981. ^{87}Sr/^{86}Sr ratios in hydrothermal waters and deposits from the East Pacific Rise at 21 N. Earth Planet. Sci. Lett. 55 (2), 229–236.

Alt, J.C., Teagle, D.A.H., 2000. Hydrothermal alteration and fluid fluxes in ophiolites and oceanic crust. In: Dilek, Y.M., Moores, E.M., Elthon, D., Nicolas, A. (Eds.), Ophiolites and Oceanic Crust: New Insights from Field Studies and the Ocean Drilling Program. Boulder, Colorado, Geological Society of America Special Paper 349, pp. 273–282.

Alt, J., Honnorez, J., Laverne, C., Emmermann, R., 1986. Hydrothermal alteration of a 1 km section through the upper oceanic crust, deep sea drilling project Hole 504B: mineralogy, chemistry, and evolution of seawater–basalt interactions. J. Geophys. Res. 91 (B10), 10309–10336.

Alt, J.C., Teagle, D., Bach, W., Halliday, A., Erzinger, J., 1996. Stable and strontium isotopic profiles through hydrothermally altered upper oceanic crust, ODP Hole 504B. In: Alt, J.C., Kinoshita, H., Stokking, L., Michael, P. (Eds.), Proc. ODP, Sci. Results, 148, College Station, TX (Ocean Drilling Program), pp. 47–70.

Andersen, D., Lindsley, D., 1988. Internally consistent solution models for Fe–Mg–Mn–Ti oxides: Fe–Ti oxides. Am. Mineral. 73 (7–8), 714–726.

Árnason, B., 1977. Hydrothermal systems in Iceland traced by deuterium. Geothermics 5 (1–4), 125–151.

Arnórsson, S., 1995. Geothermal systems in Iceland: structure and conceptual models − I. High-temperature areas. Geothermics 24, 561–602.

Bach, W., Humphris, S.E., 1999. Relationship between the Sr and O isotope compositions of hydrothermal fluids and the spreading and magma-supply rates at oceanic spreading centers. Geology 27, 1067–1070.

Bacon, J.R., Bain, D.C., 1995. Characterization of environmental water samples using strontium and lead stable isotope compositions. Environ. Geochem. Health 17 (1), 39–49.

Bargar, K.E., Fournier, R.O., 1988. Effects of glacial ice on subsurface temperatures of hydrothermal systems in Yellowstone National Park, Wyoming: fluid-inclusion evidence. Geology 16 (12), 1077–1080.

Bird, D., Spieler, A., 2004. Epidote in geothermal systems. Rev. Mineral. Geochem. 56 (1), 235–300.

Bischoff, J.L., Rosenbauer, R.J., 1984. The critical point and two-phase boundary of seawater, 200–500 C. Earth Planet. Sci. Lett. 68 (1), 172–180.

Bjarnason, I.Th., Menke, W., Flóvenz, Ó.G., Caress, D., 1993. Tomographic Image of the Mid-Atlantic Plate Boundary. J. Geophys. Res. 98 (B4), 6607–6622.

Björnsson, S., Arnorsson, S., Tomasson, J., 1970. Exploration of the Reykjanes thermal brine area. Geothermics 2 (2), 1640–1650.

Bourgeois, O., Dauteuil, O., Van Vliet-Lanoe, B., 2000. Geothermal control on flow patterns in the last glacial maximum ice sheet of Iceland. Earth Surf. Process. Landf. 25, 59–76.

Canales, J.P., Sohn, R.A., Demartin, B.J., 2007. Crustal structure of the Trans-Atlantic Geotraverse (TAG) segment (Mid-Atlantic Ridge, 26° 10′ N): implications for the nature of hydrothermal circulation and detachment faulting at slow spreading ridges. Geochem. Geophys. Geosyst. 8 (8).

Cannat, M., 1993. Emplacement of mantle rocks in the seafloor at mid-ocean ridges. J. Geophys. Res. Solid Earth 98 (B3), 4163–4172.

Casadevall, T., Ohmoto, H., 1977. Sunnyside Mine, Eureka mining district, San Juan County. Colorado; geochemistry of gold and base metal ore deposition in a volcanic environment. Econ. Geol. 72 (7), 1285–1320.

Charlou, J.L., Donval, J.P., Fouquet, Y., Jean-Baptiste, P., Holm, N., 2002. Geochemistry of high H 2 and CH 4 vent fluids issuing from ultramafic rocks at the Rainbow hydrothermal field (36 14′ N, MAR). Chem. Geol. 191 (4), 345–359.

Cole, D.R., 1983. Chemical and isotopic investigation of warm springs associated with normal faults in Utah. J. Volcanol. Geotherm. Res. 16 (1), 65–98.

Cole, D.R., Ripley, E.M., 1999. Oxygen isotope fractionation between chlorite and water from 170 to 350 °C: a preliminary assessment based on partial exchange and fluid/rock experiments. Geochim. Cosmochim. Acta 63 (3–4), 449–457.

Cole, D.R., Riciputi, L.R., Horita, J., Chacko, T., 1998. Stable isotope exchange equilibria and kinetics in mineral–fluid systems. In: Hulston, A.A. (Ed.), Water–Rock Interaction. Balkema, Rotterdam, pp. 827–830.

Dansgaard, W., 1964. Stable isotopes in precipitation. Tellus 16 (4), 436–468.

Darbyshire, F.A., Bjarnason, I.T., White, R.S., Flóvenz, Ó.G., 1998. Crustal structure above the Iceland mantle plume imaged by the ICEMELT refraction profile. Geophys. J. Int. 135 (3), 1131–1149.

Davis, A., Bickle, M., Teagle, D., 2003. Imbalance in the oceanic strontium budget. Earth Planet. Sci. Lett. 211 (1–2), 173–187.

deMartin, B.J., Sohn, R.A., Canales, J.P., Humphris, S.E., 2007. Kinematics and geometry of active detachment faulting beneath the Trans-Atlantic Geotraverse (TAG) hydrothermal field on the Mid-Atlantic Ridge. Geology 35 (8), 711–714.

Douville, E., Charlou, J.L., Oelkers, E.H., Bienvenu, P., Jove Colon, C.F., Donval, J.P., Fouquet, Y., Prieur, D., Appriou, P., 2002. The rainbow vent fluids (36 14′ N, MAR): the influence of ultramafic rocks and phase separation on trace metal content in Mid-Atlantic Ridge hydrothermal fluids. Chem. Geol. 184 (1), 37–48.

Eiler, J.M., Schiano, P., Kitchen, N., Stopler, E.M., 2000. Oxygen-isotope evidence for recycled crust in the sources of mid-ocean-ridge basalts. Nature 403, 530–534.

Elderfield, H., Greaves, M., 1981. Strontium isotope geochemistry of Icelandic geothermal systems and implications for sea water chemistry. Geochim. Cosmochim. Acta 45 (11), 2201–2212.

Elderfield, H., Schultz, A., 1996. Mid-ocean ridge hydrothermal fluxes and the chemical composition of the ocean. Annu. Rev. Earth Planet. Sci. 24 (1), 191–224.

Fisher, A., 1998. Permeability within basaltic oceanic crust. Rev. Geophys. 36 (2), 143–182.

Forester, R.W., Taylor, H.P., 1980. Oxygen, hydrogen, and carbon isotope studies of the Stony Mountain complex, western San Juan Mountains. Colorado. Econ. Geol. 75 (3), 362–383.

Fowler, A., Zierenberg, R., Schiffman, P., Marks, N., Fridliefsson, G., 2015. Evolution of fluid–rock interaction in the Reykjanes geothermal system, Iceland: evidence from Iceland Deep Drilling Project core RN-17B. J. Volcanol. Geotherm. Res. 302, 47–63. http://dx.doi.org/10.1016/j.jvolgeores.2015.06.009.

Franzson, H., Thordarson, S., Björnsson, G., Gudlaugsson, S., Richter, B., Fridleifsson, G., Thorhallsson, S., 2002. Reykjanes high-temperature field, SW-Iceland. Geology and hydrothermal alteration of well RN-10. Workshop on Geothermal Reservoir Engineering 27, pp. 233–240.

Fridleifsson, G., Ármannsson, H., Árnason, K., Bjarnason, I., Gìslason, G., 2003. Iceland deep drilling project part I: geosciences − site selection. In: Fridleifsson, G. (Ed.), Iceland Deep Drilling Project Feasibility Report, volume OS-2003-007, p. 103.

Fridleifsson, G., Blischke, A., Kristjánsson, B., Richter, B., Einarsson, G., Jónasson, H., Franzson, H., Sigurdsson, O., Danielsen, P., Jónsson, S., Thordarson, S., Thórhallsson, S., Hardardóttir, V., Egilson, T., 2005. Reykjanes well report RN-17 and RN-17ST. Technical Report ISOR-2005/007. ISOR.

Fridriksson, T., Kristjánsson, B.R., Ármannsson, H., Margrétardóttir, E., Ólafsdóttir, S., Chiodini, G., 2006. CO 2 emissions and heat flow through soil, fumaroles, and steam heated mud pools at the Reykjanes geothermal area. SW Iceland. Appl. Geochem. 21 (9), 1551–1569.

German, C.R., Lin, J., 2004. The Thermal Structure of the Oceanic Crust, Ridge-Spreading and Hydrothermal Circulation: How Well do we Understand their Inter-Connections? In: German, C.R., Lin, J., Parson, L.M. (Eds.), Mid-Ocean Ridges. American Geophysical Union, Washington, D.C. http://dx.doi.org/10.1029/148GM01

Gillis, K., Coogan, L., Pedersen, R., 2005. Strontium isotope constraints on fluid flow in the upper oceanic crust at the East Pacific Rise. Earth Planet. Sci. Lett. 232 (1), 83–94.

Graustein, W.C., Armstrong, R.L., 1983. The use of strontium-87/strontium-86 ratios to measure atmospheric transport into forested watersheds. Science 219, 289–292. http://dx.doi.org/10.1126/science.219.4582.289.

Green, G.R., Ohmoto, H., Date, J., Takahashi, T., 1983. Whole-rock oxygen isotope distribution in the Fukazawa-Kosaka area, Hokuroku district, Japan, and its potential application to mineral exploration. Econ. Geol. Monogr. 5, 395–411.

Gregory, R.T., Taylor, H.P., 1981. An oxygen isotope profile in a section of Cretaceous oceanic crust, Samail Ophiolite, Oman: evidence for δ18O buffering of the oceans by deep (>5 km) seawater-hydrothermal circulation at mid-ocean ridges. J. Geophys. Res. Solid Earth 86 (B4), 2737–2755. http://dx.doi.org/10.1029/JB086iB04p02737.

Gudmundsson, A., 1986. Mechanical aspects of postglacial volcanism and tectonics of the Reykjanes Peninsula, Southwest Iceland. J. Geophys. Res. 91, 12711–12721.

Gudmundsson, A., 1987. Geometry, formation and development of tectonic fractures on the Reykjanes Peninsula, Southwest Iceland. Tectonophysics 139 (3–4), 295–308.

Gudmundsson, A., 1990. Emplacement of dikes, sills and crustal magma chambers at divergent plate boundaries. Tectonophysics 176 (3–4), 257–275.

Hardardóttir, V., Brown, K., Fridriksson, T., Hedenquist, J., Hannington, M., Thorhallsson, S., 2009. Metals in deep liquid of the Reykjanes geothermal system, Southwest Iceland: implications for the composition of seafloor black smoker fluids. Geology 37 (12), 1103–1106.

Hardardóttir, V., Hannington, M., Hedenquist, J., Kjarsgaard, I., Hoal, K., 2010. Cu-rich scales in the Reykjanes geothermal system, Iceland. Econ. Geol. 105, 1143–1155.

Harper, G.D., Bowman, J.R., Kuhns, R., 1988. A field, chemical, and stable isotope study of subseafloor metamorphism of the Josephine ophiolite, California-Oregon. J. Geophys. Res.: Solid Earth 93 (B5), 4625–4656 (Chicago).

Harris, M., Coggon, R.M., Smith-Duque, C.E., Cooper, M.J., Milton, J.A., Teagle, D.A., 2015. Channelling of hydrothermal fluids during the accretion and evolution of the upper oceanic crust: Sr isotope evidence from ODP Hole 1256D. Earth Planet. Sci. Lett. 416, 56–66.

Hart, S.R., Blusztajn, J., Dick, H.J.B., Meyer, P.S., Muehlenbachs, K., 1999. The fingerprint of seawater circulation in a 500-meter section of ocean crust gabbros. Geochim. Cosmochim. Acta 63, 4,059–4,080. http://dx.doi.org/10.1016/S0016-7037(99)00309-9.

Hemond, Ch., Comdonines, M., Fourcade, S., Allège, C.J., Oskarsson, N., Javoy, M., 1988. Thorium, strontium and oxygen isotopic geochemistry in recent tholeiites from Iceland: crustal influence on mantle-derived magmas. Earth Planet. Sci. Lett. 87, 273–285.

Hemond, C., Arndt, N., Lichtenstein, U., Hofmann, A., Oskarsson, N., Steinthorsson, S., 1993. The heterogeneous Iceland plume-Nd–Sr–O isotopes and trace element constraints. J. Geophys. Res. 98 (B9), 15–833.

Hobbs, J.A., Yin, Q., Burton, J., Bennett, W.A., 2005. Retrospective determination of natal habitats for an estuarine fish with otolith strontium isotope ratios. Mar. Freshw. Res. 56, 655–660.

Hreinsdóttir, S., Einarsson, P., Sigmundsson, F., 2001. Crustal deformation at the oblique spreading Reykjanes Peninsula, SW Iceland: GPS measurements from 1993 to 1998. J. Geophys. Res. Solid Earth 106 (B6), 13803–13816.

Hubbard, A., Sugden, D., Dugmore, A., Norddahl, H., Pétursson, H.G., 2006. A modeling insight into the Iceland Last Glacial Maximum ice sheet. Quat. Sci. Rev. 25, 2283–2296.

Jóhannesson, H., 1989. Geology on the Reykjanes Peninsula. In: Egilsson, K. (Ed.), Icelandic, Jardfrædi á sunnanverdum Reykjanesskaga. Náttúrufrædistofnun Íslands, Reykjavík, Iceland, pp. 13–21.

Kawahata, H., Kusakabe, M., Kikuchi, Y., 1987. Strontium, oxygen, and hydrogen isotope geochemistry of hydrothermally altered and weathered rocks in DSDP hole 504B, Costa-Rica Rift. Earth Planet. Sci. Lett. 85 (4), 343–355.

Kirchner, T.M., Gillis, K.M., 2012. Mineralogical and strontium isotopic record of hydrothermal processes in the lower ocean crust at and near the East Pacific Rise. Contrib. Mineral. Petrol. 1–19.

Kokfelt, T., Hoernle, K., Hauff, F., Fiebig, J., Werner, R., Garbe-Schönberg, D., 2006. Combined trace element and Pb–Nd–Sr–O isotope evidence for recycled oceanic crust (upper and lower) in the Iceland mantle plume. J. Petrol. 47 (9), 1705–1749.

Lonker, S., Franzson, H., Kristmannsdottir, H., 1993. Mineral-fluid interactions in the Reykjanes and Svartsengi geothermal systems, Iceland. Am. J. Sci. 293 (7), 605–670.

Marks, N., Schiffman, P., Zierenberg, R., Franzson, H., Fridleifsson, G., 2010. Hydrothermal alteration in the Reykjanes geothermal system: Insights from Iceland Deep Drilling Program well RN-17. J. Volcanol. Geotherm. Res. 189, 172–190.

Marks, N., Schiffman, P., Zierenberg, R.A., 2011. High-grade contact metamorphism in the Reykjanes geothermal system: implications for fluid–rock interactions at mid-oceanic ridge spreading centers. Geochem. Geophys. Geosyst. 12, Q08007. http://dx.doi.org/10.1029/2011GC003569.

Matsuhisa, Y., Goldsmith, J.R., Clayton, R.N., 1979. Oxygen isotopic fractionation in the system quartz–albite–anorthite–water. Geochim. Cosmochim. Acta 43, 1131–1140.

McCulloch, M., Gregory, R., Wasserburg, G., Taylor Jr., H., 1980. A neodymium, strontium, and oxygen isotopic study of the Cretaceous Samail Ophiolite and implications for the petrogenesis and seawater-hydrothermal alteration of oceanic crust. Earth Planet. Sci. Lett. 46 (2), 201–211.

Menke, W., 1999. Crustal isostasy indicates anomalous densities beneath Iceland. Geophys. Res. Lett. 26 (9), 1215–1218.

Michard, G., Albarède, F., Michard, A., Minster, J., Charlou, J., Tan, N., 1984. Chemistry of solutions from the 13°N East Pacific Rise hydrothermal site. Earth Planet. Sci. Lett. 67 (3), 297–307.

Millot, R., Ásmundsson, R., Négrel, P.H., Sanjuan, B., Bullen, T.D., 2009. Multi-isotopic (H, O, C, S, Li, B, Si, Sr, Nd) approach for geothermal fluid characterization in Iceland. Geochim. Cosmochim. Acta (Suppl. 73), 883.

Mottl, M., 1983. Metabasalts, axial hot springs, and the structure of hydrothermal systems at mid-ocean ridges. Geol. Soc. Am. Bull. 94 (2), 161–180.

Mottl, M., 2003. Partitioning of energy and mass fluxes between mid-ocean ridge axes and flanks at high and low temperature. In: Halbach, P.E., Tunnicliffe, V., Hein, J.R. (Eds.), Energy and Mass Transfer in Marine Hydrothermal Systems. Dahlem UP, Berlin, pp. 271–286.

Mottl, M., Holland, H., 1978. Chemical exchange during hydrothermal alteration of basalt by seawater — I. Experimental results for major and minor components of seawater. Geochim. Cosmochim. Acta 42 (8), 1103–1115.

Muehlenbachs, K., Clayton, R., 1972. Oxygen isotope studies of fresh and weathered submarine basalts. Can. J. Earth Sci. 9 (2), 172–184.

Muehlenbachs, K., Andersson Jr., A.T., Sigvaldson, G.E., 1974. Low-O18 basalts from Iceland. Geochim. Cosmochim. Acta 38, 577–588.

Murton, B., Taylor, R., Thirlwall, M., 2002. Plume–ridge interaction: a geochemical perspective from the Reykjanes Ridge. J. Petrol. 43 (11), 1987–2012.

Ólafsson, J., Riley, J., 1978. Geochemical studies on the thermal brine from Reykjanes (Iceland). Chem. Geol. 2, 219–237.

Palmer, M., Edmond, J., 1989. The strontium isotope budget of the modern ocean. Earth Planet. Sci. Lett. 92 (1), 11–26.

Pearce, J., 2008. Geochemical fingerprinting of oceanic basalts with applications to ophiolite classification and the search for Archean oceanic crust. Lithos 100 (1–4), 14–48.

Peate, D., Baker, J., Jakobsson, S., Waight, T., Kent, A., Grassineau, N., Skovgaard, A., 2009. Historic magmatism on the Reykjanes Peninsula, Iceland: a snap-shot of melt generation at a ridge segment. Contrib. Mineral. Petrol. 157 (3), 359–382.

Pope, E., Bird, D., Arnórsson, S., Fridriksson, T., Elders, W., Fridleifsson, G., 2009. Isotopic constraints on ice age fluids in active geothermal systems: Reykjanes, Iceland. Geochim. Cosmochim. Acta 73, 4468–4488.

Ravizza, G., Blusztajn, J., Von Damm, K.L., Bray, A.M., Bach, W., Hart, S.R., 2001. Sr isotope variations in vent fluids from 9°46′–9°54′N East Pacific Rise: evidence of a non-zero-Mg fluid component. Geochim. Cosmochim. Acta 65 (5), 729–739.

Salters, V., Stracke, A., 2004. Composition of the depleted mantle. Geochem. Geophys. Geosyst. 5, Q05B07. http://dx.doi.org/10.1029/2003GC000597.

Sharp, Z., 1990. A laser-based microanalytical method for the in-situ determination of oxygen isotope ratios of silicates and oxides. Geochim. Cosmochim. Acta 54 (5), 1353–1357.

Singh, S.C., Crawford, W.C., Carton, H., Seher, T., Combier, V., Cannat, M., Canales, J.P., Düsünür, D., Escartin, J., Miranda, J.M., 2006. Discovery of a magma chamber and faults beneath a Mid-Atlantic Ridge hydrothermal field. Nature 442 (7106), 1029–1032.

Spooner, E., Chapman, H., Smewing, J., 1977. Strontium isotopic contamination and oxidation during ocean floor hydrothermal metamorphism of the ophiolitic rocks of the Troodos Massif, Cyprus. Geochim. Cosmochim. Acta 41 (7), 873–877.

Staples, R.K., White, R.S., Brandsdóttir, B., Menke, W., Maguire, P.K., McBride, J.H., 1997. Faeroe-Iceland Ridge Experiment 1. Crustal structure of northeastern Iceland. J. Geophy. Res. Solid Earth (1978–2012) 102 (B4), 7849–7866.

Stracke, A., Zindler, A., Salters, V., McKenzie, D., Blichert-Toft, J., Albarède, F., Gronvold, K., 2003. Theistareykir revisited. Geochem. Geophys. Geosyst. 4 (2), 8507. http://dx.doi.org/10.1029/2001GC000201.

Sveinbjornsdottir, A.E., Coleman, M.L., Yardley, B.W.D., 1986. Origin and history of hydrothermal fluids of the Reykjanes and Krafla geothermal fields, Iceland. Contrib. Mineral. Petrol. 94 (1), 99–109. http://dx.doi.org/10.1007/BF00371231.

Taylor, H., 1968. The oxygen isotope geochemistry of igneous rocks. Contrib. Mineral. Petrol. 19 (1), 1–71.

Taylor, H., 1974. The application of oxygen and hydrogen isotope studies to problems of hydrothermal alteration and ore deposition. Econ. Geol. 69 (6), 843–883.

Taylor Jr, H.P., 1979. Oxygen and hydrogen isotope relationships in hydrothermal mineral deposits. In: Barnes, H.L. (Ed.), Geochem. Hydrothermal Ore Deposits 1979. Wiley, pp. 236–277.

Thordarson, T., Larsen, G., 2007. Volcanism in Iceland in historical time: volcano types, eruption styles and eruptive history. J. Geodyn. 43 (1), 118–152.

Thurnherr, A.M., Richards, K.J., 2001. Hydrography and high-temperature heat flux of the Rainbow hydrothermal site (36 14′ N, Mid-Atlantic Ridge). J. Geophy. Res. Oceans (1978–2012) 106 (C5), 9411–9426.

Tómasson, J., Kristmannsdóttir, H., 1972. High temperature alteration minerals and thermal brines, Reykjanes, Iceland. Contrib. Mineral. Petrol. 36 (2), 123–134.

Valley, J., Kitchen, N., Kohn, M., Niendorf, C., Spicuzza, M., 1995. UWG-2, a garnet standard for oxygen isotope ratios: strategies for high precision and accuracy with laser heating. Geochim. Cosmochim. Acta 59 (24), 5223–5231.